Journal of Environmental Management 357 (2024) 120787

Contents lists available at ScienceDirect

Journal of Environmental Management

journal homepage: www.elsevier.com/locate/jenvman

Research article

Multi-hazard assessment of climate-related hazards for European coastal cities

Emilio Laino [a,*], Gregorio Iglesias [a,b]

[a] School of Engineering and Architecture & Environmental Research Institute, University College Cork, Cork, Ireland
[b] University of Plymouth, School of Engineering, Computing and Mathematics, Marine Building, Drake Circus, United Kingdom

ARTICLE INFO

Handling editor: Jason Michael Evans

Keywords:
Climate change impacts
Coastal hazards
Climate-related hazards
Coastal cities
Multi-hazard assessment
Risk assessment

ABSTRACT

The assessment of risk posed by climate change in coastal cities encompasses multiple climate-related hazards. Sea-level rise, coastal flooding and coastal erosion are important hazards, but they are not the only ones. The varying availability and quality of data across cities hinders the ability to conduct holistic and standardized multi-hazard assessments. Indeed, there are far fewer studies on multiple hazards than on single hazards. Also, the comparability of existing methodologies becomes challenging, making it difficult to establish a cohesive understanding of the overall vulnerability and resilience of coastal cities. The use of indicators allows for a standardized and systematic evaluation of baseline hazards across different cities. The methodology developed in this work establishes a framework to assess a wide variety of climate-related hazards across diverse coastal cities, including sea-level rise, coastal flooding, coastal erosion, heavy rainfall, land flooding, droughts, extreme temperatures, heatwaves, cold spells, strong winds and landslides. Indicators are produced and results are compared and mapped for ten European coastal cities. The indicators are meticulously designed to be applicable across different geographical contexts in Europe. In this manner, the proposed approach allows interventions to be prioritized based on the severity and urgency of the specific risks faced by each city.

1. Introduction

Coastal cities around the world are experiencing unprecedented growth and development, fuelled by urbanization and economic activities (Neumann et al., 2015). However, this expansion is unfolding in the shadow of an escalating threat – the increasing frequency and severity of climate-related hazards, a consequence of the rapidly changing climate (Dale et al., 2001; Knutson et al., 2010; Sahoo and Bhaskaran, 2018; Zhang et al., 2023). As we journey further into the 21st century, the global population exposed to mean and Extreme Sea Level (ESL) events is poised to grow significantly, leading to a surge in research endeavours aimed at comprehending the repercussions of climate change on coastal communities (Kulp and Strauss, 2019; Lima and Bonetti, 2020; Oppenheimer et al., 2019; Wong et al., 2014). In Europe, this issue is of particular concern, as the continent's densely populated coastal areas serve as hubs for economic activities (Laino and Iglesias, 2023a). The looming threats of sea-level rise and temperature increase are poised to inundate wetlands, erode shorelines, exacerbate coastal flooding during storms, and usher in complex climatic changes (Barredo, 2007; Hosseinzadehtalaei et al., 2020; Vousdoukas et al., 2017). These changes cast long shadows over tidal deltas, coastal plains, sandy beaches, and estuaries (Ghorai and Sen, 2015; J Bergillos et al., 2019; Khojasteh et al., 2022), affecting both human and ecological values (Bergillos et al., 2020a; García et al., 2020; Rodriguez-Delgado et al., 2020).

In the case of coastal cities in Europe, coastal storms represent the primary climate-related hazard, leading to destructive Extreme Sea Levels (ESLs), coastal flooding, and coastal erosion (J Bergillos et al., 2019; Rodriguez-Delgado et al., 2020; Sardella et al., 2020). Projections indicate that ESLs will rise along European coastlines, with notable regional variations (Antunes et al., 2019; Howard et al., 2019; Lang and Mikolajewicz, 2020; Lionello et al., 2021; Luque et al., 2021; Vousdoukas et al., 2017; Wiśniewski et al., 2011). The North Sea region, the Baltic Sea, the Atlantic coasts of the United Kingdom and Ireland are expected to experience the most substantial changes, while less severe changes are foreseen along the southwestern European coasts. Other climate-related hazards are anticipated to increase in frequency and intensity in the European continent, notably those related to heatwaves, droughts, and heavy precipitation events (Forzieri et al., 2017; Kovats et al., 2014). This increase could also lead to a surge in fatalities, primarily driven by an increase in heatwaves, especially in southern

* Corresponding author.
E-mail address: elaino@ucc.ie (E. Laino).

https://doi.org/10.1016/j.jenvman.2024.120787
Received 17 January 2024; Received in revised form 14 March 2024; Accepted 27 March 2024

Europe. While progress has been made in addressing these climate change challenges, numerous European cities necessitate increased efforts to mitigate the most severe impacts (Salvia et al., 2021; Vijaya-VenkataRaman et al., 2012).

The concept of "multi-hazard assessment (MHA)" has acquired broad acceptance to refer to the consideration of the multiple hazards that have the potential to affect a particular area, since its first appearance in the United Nations' Agenda 21 for sustainable development (UNEP, 1992), and the continuous use of this term in posterior United Nations' events (e.g., Johannesburg Plan (UN, 2002) and the Hyogo Framework for Action (UN-ISDR, 2005; Wang et al., 2020). In general, multi-hazard approaches consider the interrelationships between the most relevant hazards in the study area (Gupta et al., 2020). These interrelationships usually include the simultaneity or the interdependency between the occurrence and impact of various hazards (Gill and Malamud, 2014; Kappes et al., 2012). The conception of the term multi-hazard in UNEP 1992 and its subsequent reinterpretations are also intimately related to the framework of vulnerability and risk assessment. Nowadays, numerous well-established approaches are accessible for most hazards when these are considered alone, but a significantly smaller number of methodologies deal with multiple hazards (Kappes et al., 2012).

Gallina et al. (2016) have reviewed existing MHA concepts and tools applied by organisations and projects, showing that existing MHAs typically fail to take into account the effects of climate change and to provide a joint understanding of climate impacts, spatial visualization, comparison between, and communication to, end-users. Most of the popular MHAs are not developed to assess the relationship between climate-related events and coastal cities (Buriks et al., 2004; Genovese et al., 2005; Lavalle et al., 2006). Nevertheless, there are examples of proposals of MHA intended for coastal areas analysing climate-related events (Gallina et al., 2020; Godwyn-Paulson et al., 2022; Thakur and Mohanty, 2023). In general, these approaches apply variations of the Coastal Vulnerability Index (CVI) and other existing indices (Ahsan and Warner, 2014; Gornitz, 1991; Rodriguez and Young, 2006). Other existing methodologies cover some climate-related hazard; however, these approaches do not focus on coastal cities (Elia et al., 2023; Pourghasemi et al., 2019; Rusk et al., 2022). It has been observed that the scope of the MHRAs developed for coastal cities is usually limited to coastal hazards (namely, storms, storm surges, coastal and pluvial flooding, and coastal erosion) and do not consider other climate-related hazards common to inland cities, such as heatwaves, cold spells, droughts, landslides and forest fires (Malakar et al., 2021; Rosendahl Appelquist and Balstrøm, 2015; Serafim et al., 2019). Also, the geographical coverage of these approaches may be limited (Laino and Iglesias, 2023b). An approach is lacking that permits a standardized and systematic MHA framework at European level, including all kind of climate-related hazards – not only those specific to coastal areas.

Altogether, the current state of multi-risk assessments, including MHA, reveals several critical deficiencies in the field (Curt, 2021). First, there is a notable absence of adequate decision support tools, which hinders effective risk management strategies. Additionally, the integration of practices for multi-risk governance is lacking, with minimal collaboration among diverse risk-related communities. The communication of assessment results poses a significant obstacle to successful multi-risk management efforts. Furthermore, the consideration of diverse temporal hazard scenarios, particularly those associated with global changes, presents an additional challenge that necessitates comprehensive attention and improvement in the domain of multi-risk assessments (Gallina et al., 2016).

In this context, indicator-based approaches represent a fundamental methodology for articulating the multifaceted nature of climate-related hazards (Birkmann et al., 2006; Klein and Nicholls, 1999). These approaches employ a set of independent variables to characterize key aspects of such hazards, including storm characteristics, wave regimes, sea-level changes, precipitation patterns, and temperature fluctuations, among others (Frazier et al., 2013; Lung et al., 2013; Mclaughlin and Cooper, 2010). Notably, these indicators can be occasionally aggregated to form a composite index, offering a summarized view of the overall hazard scenario (Nicholls et al., 2006). This methodology not only facilitates a nuanced assessment of the various dimensions of hazard but also integrates these assessments within a coherent and standardized evaluation framework, thereby enhancing comparability and interpretability across different cases and hazard types (Papathoma-Köhle et al., 2016).

Despite their widespread application and inherent strengths, it is important to acknowledge that the most popular indicator-based methodologies often exhibit limitations in their scope, typically concentrating on a select range of hazards or specific vulnerability parameters (Cutter et al., 2003). Common focal areas include coastal flooding, coastal erosion, physical vulnerability assessments, and the impacts on ecosystems (Baccini et al., 2009; Gallina et al., 2020; Murray et al., 2021). This specialization, while beneficial for in-depth analysis of particular hazards, may overlook the interdependencies and cumulative effects of multiple hazards that concurrently affect coastal cities (Laurien et al., 2022).

To address this gap, the methodology seeks to expand the traditional scope of indicator-based approaches by incorporating a comprehensive set of hazards relevant to coastal cities, thereby providing a more holistic view of the risk landscape. In doing so, it is recognized the necessity of adapting and refining existing methodologies to meet the specific requirements of the assessment. Drawing on the foundational work of researchers such as Klein and Nicholls (1999) and Nicholls et al. (2006) who have emphasized the importance of integrating diverse hazard indicators into coastal vulnerability assessments, the approach aims to bridge the existing methodological divide. By doing so, it is ensured that the MHA framework remains flexible and adaptable, capable of capturing the complex interplay of climate-related hazards that threaten European coastal cities.

Furthermore, the adoption of an indicator-based approach underscores the commitment for developing a methodology that is not only scientifically rigorous but also practically applicable. By carefully selecting indicators that are relevant, measurable, and sensitive to the specific contexts of European coastal cities, policymakers and practitioners are provided with a valuable tool that allows the comparison of a wide variety of climate-related hazards in practically any coastal city in Europe. In connection with the aforementioned, the intention is also to develop a systematic and standardized methodology to discern in which cities it is more crucial to continue the study in more detail. For this reason, the indicator-based approach proposed allows for the results to be refined through incremental improvement in the accuracy of indicators. Ultimately, this approach is also designed to be flexible and not excessively complex, in order to facilitate its use in collaboration with coastal communities.

2. Materials and methods

2.1. Case studies

The selection of the study cities ensures a wide representation of the geographical and climatic diversity of Europe, enabling a comprehensive analysis of climate-related hazards across different coastal environments. These cities were selected in alignment with the objectives of the 'Smart control of the climate resilience in European coastal cities' (SCORE) project, covering ten diverse cities: Sligo and Dublin (Ireland); Vilanova i la Geltrú, Benidorm, and Oarsoaldea (Spain); Oeiras (Portugal); Massa (Italy); Piran (Slovenia); Gdansk (Poland); and Samsun (Türkiye).

This selection facilitates the study to span a broad spectrum of climate change challenges, from variations in risk exposure to differing urbanization levels, thereby providing a framework for evaluating not only different scenarios of hazard, but also of coastal vulnerability and resilience. The choice is further justified by the varying degrees of

existing research on the impacts of climate change in these areas (Laino and Iglesias, 2023c), which allows the study to build upon and contribute to the existing body of knowledge with new insights into hazard assessment methodologies.

Moreover, the involvement of these cities in the SCORE project not only grants access to rich datasets and localized contexts but also positions the methodology for practical application. This integration promises to enhance the decision-making process for urban planning and climate adaptation measures, directly contributing to the advancement of climate resilience in European coastal cities. Through this approach, the research directly responds to the urgent need for actionable insights in the face of escalating climate threats, ensuring that the findings have both scientific and practical relevance.

In this vein, essential geographic information vital for the comprehensive analysis of the target coastal cities was obtained by means of robust data acquisition techniques. The acquisition of city coordinates was accomplished through OpenStreetMap data, facilitated by the geopy library – a renowned geolocation tool. The Local Administrative Units (LAU) dataset sourced from Eurostat, a reputable repository of European statistical data, was employed to further refine the geographical characterization of the coastal cities. For the specific case of Turkey, geographical data aligned with the Nomenclature of Territorial Units for Statistics (NUTS) 2021 classification from Eurostat was employed. In this context, the territorial boundary of the province of Samsun, delineated at the NUTS 3 level, was utilized to represent the coastal area of the city of Samsun.

These meticulously obtained city coordinates and boundaries served as the foundational geographic references that underpinned the subsequent analyses (Table 1). The approach seamlessly integrated a bespoke Python script with Geographic Information System (GIS) data, enabling the automated retrieval of latitude and longitude coordinates. This methodological synergy assured precision and consistency in the geographical data, setting the stage for the calculation of various indicators elaborated upon in subsequent sections of the paper.

Table 1
Geographic characterisation of coastal cities.

Coastal city	Coordinates (Latitude, Longitude)	Geographical extents (LAU or NUTS names)
Sligo	(54.192986, −8.730543)	Sligo-Drumcliff; Sligo-Strandhill
Dublin	(53.349380, −6.260559)	Artane-Whitehall; Ballyfermot-Drimnagh; Ballymun-Finglas; Cabra-Glasnevin; Clontarf; Donaghmede; Kimmage-Rathmines; North Inner City; Pembroke; South East Inner City; South West Inner City
Vilanova i la Geltrú	(41.224199, 1.725633)	Vilanova i la Geltrú
Benidorm	(38.540626, −0.129093)	Benidorm
Oarsoaldea	(43.312527, −1.898613)	Pasaia; Lezo; Errenteria; Oiartzun
Oeiras	(38.712497, −9.271300)	Porto Salvo; Barcarena; União das freguesias de Carnaxide e Queijas; União das freguesias de Oeiras e São Julião da Barra, Paço de Arcos e Caxias; União das freguesias de Algés, Linda-a-Velha e Cruz Quebrada-Dafundo
Massa	(44.035932, 10.139552)	Massa
Piran	(45.528492, 13.568449)	Piran/Pirano
Gdańsk	(54.348291, 18.654023)	Gdańsk
Samsun	(41.230356, 35.968334)	Samsun (NUTS3)

2.2. Selection of indicators

The selection of indicators, summarized in Table 2, was based on a synthesis of authoritative sources and recent research findings tailored to the European context. First, the Sixth Assessment Report by the IPCC served as a foundational reference (Ranasinghe et al., 2021), offering a comprehensive classification of climate-related events, which underpins the understanding of potential hazards affecting coastal environments.

Second, further refinement of the indicator selection was informed by the European Topic Centre on Climate Change Impacts, Vulnerability, and Adaptation, which evaluates and prioritizes climate-related hazard indices for Europe based on their significance, adaptation relevance, data availability, and data robustness (Crespi et al., 2020). This prioritization aims to produce indicators that can be applied homogeneously and systematically in the European coastal context.

Finally, the approach aligns with and builds upon recent studies that employ hazard indicators. Lung et al. (2013) and Hincks et al. (2023) analyse a range of hazards including coastal, temperature extremes, precipitation, flooding, drought and landslide for regional risk assessments in Europe. The collaborative research conducted by Laino and Iglesias (2023c), which combines a review of existing literature with insights from local stakeholders in the study cities, provides critical insights into the local perceptions of climate-related hazards. This alignment with established research ensures that the methodology is not only grounded in the latest scientific understanding but also addresses the specific challenges and local concerns faced by coastal cities in adapting to climate change.

2.3. Sea-level rise

Sea-level rise is the sustained increase in the average height of the ocean's surface over a specified period, primarily driven by the thermal expansion of seawater and the melting of polar ice caps and glaciers. In the context of coastal cities hazard assessments, sea-level rise is a critical parameter to consider, as it poses a substantial and escalating risk to these urban areas (Petrosillo et al., 2006). It may lead to coastal flooding, erosion, and intensified storm surge impacts, significantly amplifying the vulnerability of these regions to natural disasters and necessitating robust adaptation and mitigation strategies to safeguard both human populations and critical infrastructure (Paranunzio et al., 2021).

Sea-level change rates have been estimated using the NASA Sea-Level Projection Tool (Garner et al., 2021; Intergovernmental Panel on Climate Change (IPCC), 2023; Kopp et al., 2023). Values are measured for the year 2020 under the SSP2-4.5 scenario (relative to a 1995–2014 baseline), including global and regional contributions from changes in steric conditions, Greenland and Antarctic ice sheets, glaciers, ocean dynamics, gravitational-rotational-deformational effects of the Earth, land-water storage and glacial isostatic adjustment and other drivers of vertical land motion.

2.4. Storm surge, wave regime and tidal range

The addition of storm surge, waves and tides to regional sea-level rise results in ESL (IPCC, 2021). Indicators for these parameters have been measured from the downscaled meteorological forcing from the ERA5 climate reanalysis for the period 2001–2017 through the application *Indicators of water level change for European coasts in the* 21st *Century Wave* (Caires and Yan, 2020; Hersbach et al., 2020; Yan et al., 2020). Results for each indicator are averaged from the stations located within a circle centred in the coastal city of radii 0.5° (circa 55.6 km) for Sligo, Dublin, Gdańsk and Samsun and 0.2° (circa 22.2 km) for the rest of cities using a regular latitude-longitude grid with a spatial resolution 0.1°.

The significant wave height (H_s) and peak wave period (T_p) are key descriptors for characterizing wave conditions in marine and coastal environments. Hs quantifies the average height of the highest one-third

Table 2
Summary of indicators, including units and spatial and temporal resolution and coverage.

Indicator (units)	Spatial resolution and coverage	Temporal resolution and coverage	Data source
MSL rate (mm/year)	1-degree grid; global	Decade, 2020 relative to a 1995–2014 baseline	NASA Sea-Level Projection Tool (Garner et al., 2021; Intergovernmental Panel on Climate Change (IPCC), 2023; Kopp et al., 2023)
Storm surge level (m)	0.1-degree grid; Europe	Value corresponding to the 50th percentile of the 50-year return period from 2001 to 2017 ERA5 reanalysis	Indicators of water level change for European coasts in the 21st Century (Caires and Yan, 2020; Hersbach et al., 2020; Yan et al., 2020)
Significant wave height (m)	0.1-degree grid; Europe	Average value between the 90th and 100th percentiles from 2001 to 2017 ERA5 reanalysis	Indicators of water level change for European coasts in the 21st Century Wave (Caires and Yan, 2020; Hersbach et al., 2020; Yan et al., 2020)
Peak wave period (s)	0.1-degree grid; Europe	Average value between the 90th and 100th percentiles from 2001 to 2017 ERA5 reanalysis	Indicators of water level change for European coasts in the 21st Century Wave (Caires and Yan, 2020; Hersbach et al., 2020; Yan et al., 2020)
Annual highest high tide (m)	0.1-degree grid; Europe	Value corresponding to the 50th percentile of the 50-year return period from 2001 to 2017 ERA5 reanalysis	Indicators of water level change for European coasts in the 21st Century Wave (Caires and Yan, 2020; Hersbach et al., 2020; Yan et al., 2020)
Coastal flooding extents (%)	100-m; most Europe	Values corresponding to the 50-year return period and 36-h duration storm	ECFAS Pan-EU Flood Catalogue (Le Gal et al., 2022, 2023)
LECZ area (%)	3-arc-seconds; global	Single values reflecting conditions pre-2017	MERIT DEM (Yamazaki et al., 2017)
Coastline length undergoing erosion (%)	200 m; Europe	Single values reflecting conditions up to the early 2000s	Eurosion (Lenôtre et al., 2004)
Land flooding area (%)	100 m; Europe and its surrounding areas	Values for the 100-year return period based on daily river flows between 1990 and 2016	River flood hazard maps for Europe and the Mediterranean Basin region (Dottori et al., 2021)
Heavy rainfall frequency (day/year)	0.25-degree; Europe	Day; 1981–2019	Extreme precipitation risk indicators for Europe and European cities from 1950 to 2019 (Hersbach et al., 2020; Mercogliano et al., 2021)
Drought frequency (month/year)	1-degree; global	Month; 1981–2020	Global Drought Observatory (European Commission and Joint Research Centre (JRC), 2021)
Extreme high temperature threshold (°C)	0.25-degree; Europe	Day; 1981–2020	European Drought Observatory (Lavaysse et al., 2018)
Extreme low temperature threshold (°C)	0.25-degree; Europe	Day; 1981–2020	European Drought Observatory (Lavaysse et al., 2018)
Heatwave frequency (day/year)	0.25-degree; Europe	Day; 1981–2020	European Drought Observatory (Lavaysse et al., 2018)
Cold spell frequency (day/year)	0.25-degree; Europe	Day; 1981–2020	European Drought Observatory (Lavaysse et al., 2018)
Strong winds frequency (event/year)	1 km; 20W-35E, 35N–70N regular latitude-longitude grid	Hour; 1981–2020	Winter windstorm indicators for Europe from 1979 to 2021 derived from reanalysis (Copernicus Climate Change Service and Climate Data Store, 2022; Hersbach et al., 2020)
Landslide-prone area (%)	200 m; Europe	Single values reflecting conditions pre-2018	ELSUS v2 (Wilde et al., 2018)

of waves in a given wave dataset. T_p is a measure of the time interval between successive wave crests passing a fixed point. It represents the dominant or most frequent time period between individual wave crests in a wave train. Values corresponding to the average between 90th and 100th percentiles for H_s and T_p were selected as these offer a compromise between conservatism and practicality. They account for wave conditions that are higher than most observed conditions but do not go to the extreme levels of the 99th and 100th percentiles.

The Surge Level (SL) and Annual Highest High Water (AHHW) complete the selection of indicators for the high-level characterisation of ESLs. Storm surge (and consequently SL) is a temporary and abnormal rise in sea level, typically associated with storm conditions. It results from a combination of factors, including strong winds, atmospheric pressure changes, and the geomorphology of the coastline. AHHW includes the contribution from the statistical annual highest hide tide, mean sea level and sea-level rise, but does not account for storm surge caused by atmospheric forcing. The 50-year return period and 50th percentile have been utilized as they address the potential for rare but significant surge events and are typically considered for critical infrastructure and long-term urban planning. The 50th percentile represents a neutral approach corresponding to the median surge level within the 50-year return period.

2.5. Coastal flooding extents and low-elevation coastal zone

The examination of areas vulnerable to coastal flooding is integral to delineating the scope of flood risk. Such analysis is foundational for identifying prevailing flood risk patterns and temporal trends, which are essential for conducting thorough risk assessments and formulating strategic planning and mitigation efforts. To this end, two indicators were developed based on most recent coastal flooding maps and the concept of Low-Elevation Coastal Zones.

The European Coastal Flood Awareness System (ECFAS) Pan-EU Flood Catalogue was employed as a primary data source to quantify the extent of areas susceptible to coastal flooding within the study cities (Le Gal et al., 2022, 2023). This comprehensive repository offers detailed mappings of coastal flood projections across Europe. These projections are based on 15 scenarios that simulate synthetic storms of varying intensities and durations. The scenarios are constructed around Total Water Levels (TWLs) for return periods extending from 2 to 50 years, coupled with storm durations spanning 12, 24, and 36 h, and are

rendered at a spatial resolution of 100 m, ensuring detailed and accurate delineation of flood extents.

For the purpose of this study, the most conservative scenario—representing a 50-year return period and a 36-h storm duration—was selected. This decision was aimed to capture the full spectrum of potential flood impacts, thereby facilitating a comprehensive assessment of urban areas at heightened risk and also to enhance the reliability of the findings in supporting the development of adaptive strategies and policy interventions.

The Low Elevation Coastal Zone (LECZ) is commonly utilized as an indicator to assess the vulnerability of coastal areas to a range of climate-related hazards in the context of coastal cities (Fang et al., 2020). It is defined as a contiguous geographical area situated in close proximity to the coastline, with an elevation less than 10 m above Mean Sea Level (MSL). LECZs hold particular significance in hazard assessment due to their typical characteristics of high population density and economic development, as well as their close proximity to the sea, rendering them susceptible to various coastal hazards.

For the purpose of this study, LECZ areas were systematically determined for each coastal city under investigation. This determination was facilitated by employing the Multi-Error-Removed Improved-Terrain Digital Elevation Model (MERIT DEM), a global digital elevation model characterized by a high level of accuracy (MacManus et al., 2021; Yamazaki et al., 2017). The MERIT DEM boasts a spatial resolution of 3 arc-seconds, equivalent to approximately 90 m at the Equator, and ±2 m of vertical resolution. The MERIT DEM is constructed by amalgamating data from various existing spaceborne DEMs, including the NASA SRTM3 DEM v2.1, JAXA AW3D-30m DEM v1, and Viewfinder Panoramas' DEM. Furthermore, it is complemented by other pertinent datasets in order to minimize multiple error components.

To further assess coastal vulnerability, the LECZ areas were delineated using the MERIT DEM data and subsequently compared to the overall coastal city area. This assessment provided a valuable metric for expressing the extent of coastal exposure, effectively quantifying the vulnerability of these urban coastal regions to climate-related hazards.

2.6. Coastline length under erosion

Coastal erosion refers to the net removal of material from one coastal location to another, influenced by various natural factors including storm surge, changes in wave energy, sediment supply, and sea-level rise (Bergillos et al., 2020a). The inevitability of coastal erosion often culminates in shoreline retreat, be it gradual due to sea-level rise or episodic due to ESLs or coastal flooding (Dawson et al., 2009; J Bergillos et al., 2019).

Coastline erosion trends (erosion, aggradation, stability) have been analysed for each coastal city, with the exception of Samsun, using data from Eurosion database (Eurosion, 2004). The European coastal database Eurosion contains information regarding shoreline evolution over the 1990s with a scale of 1:100,000. In particular, coastline segments are classified according to the observed erosional trend. These segments are classified in four categories: erosion, aggradation, stable or undetermined. Categories of erosion, aggradation and stable directly refer to the erosional trend for each coastline segment, and undetermined applies when no data are available. The total coastline lengths under erosion were computed and expressed as a percentage of the total coastline length for each study city.

2.7. Heavy precipitation and land flooding

Land flooding, defined as the inundation of terrestrial areas by water resulting from various factors, including heavy rainfall, storm surges, rising sea levels, and river flooding, holds a paramount role in the hazard assessment of coastal cities, significantly augmenting their risk profiles (Beden and Ulke, 2020). This can lead to severe consequences, such as property damage, infrastructure disruption, and threats to ecosystems and human lives, making it a critical factor in the evaluation and mitigation of hazards in coastal urban environments (Cai et al., 2011).

Heavy rainfall events refer to periods of intense and excessive precipitation, characterized by a significant and often rapid accumulation of rainfall within a specific geographic area or time frame, exceeding the average or expected rainfall amounts for that region or period (Chen et al., 2022; Ülke Keskin et al., 2018). In this study, heavy rainfall events have been characterized by calculating the frequency of daily rainfall exceeding 20 mm, due to their consistency for cross-city comparisons, relevance in areas with limited soil infiltration, utility in assessing infrastructure resilience, effectiveness in risk communication, and swift risk identification. The underlying rainfall data used to calculate these values are derived from the ERA5 reanalysis, encompassing a spatial resolution of $0.25^\circ \times 0.25^\circ$ for the period 1979–2019, as per Mercogliano et al. (2021).

The flood extents represent the areas susceptible to flooding and have been extracted for the coastal cities using data sourced from the "River flood hazard maps for Europe and the Mediterranean Basin region" from the Joint Research Centre dataset (Dottori et al., 2021). Specifically, the flood extents correspond to events with a 100-year return period and spatial resolution of 100 m, thus providing a robust perspective on the potential severity of flooding in these regions and detailed and precise mapping of flood-prone areas. Flood-prone areas are expressed as a percentage of the total coastal city area for subsequently comparison.

2.8. Droughts

Droughts can be defined as extreme events related to climate, marked by enduring and significantly dry weather patterns that upset the balance of hydrological processes, causing widespread impacts (Dąbrowska et al., 2023; García-Herrera et al., 2019; Vicente-Serrano et al., 2020). Such conditions are often associated with reduced precipitation, soil moisture, and water storage levels, which contribute to the categorization of drought into three types, namely meteorological, agricultural, and hydrological drought, respectively.

The Standard Precipitation Index with a 3-month aggregation window (SPI-3) is a widely recognized and accepted indicator for meteorological drought assessment (WMO, 2012). In this study, drought events were evaluated using this indicator, specifically, the number of drought months within the period spanning from 1981 to 2020 for each city. To derive this indicator, the geographic coordinates of the cities mentioned earlier are employed. The quantification of drought months was accomplished through the utilization of the SPI-3 data from EDO, with a spatial resolution of 1° and calculated over the reference period of 1991–2020 (European Commission and Joint Research Centre (JRC), 2021; McKee et al., 1993). Drought months are considered those with SPI-3 falls below −1.

2.9. Temperature extremes, heatwaves and cold spells

Extreme temperatures, which hold significant relevance for sectors such as agriculture, forestry, fire management, public health, and infrastructure planning, were systematically quantified (Mitsopoulos et al., 2019; Mitsopoulos and Mallinis, 2017). To this end, relative thresholds were established based on daily temperature data. These thresholds were carefully designed to capture the unique characteristics and variations of the local climate, thus providing a more refined and context-specific evaluation of extreme temperatures, as opposed to the use of absolute temperature values (Paranunzio et al., 2021). Furthermore, this approach facilitated the precise identification and differentiation of various extreme temperature events, including heatwaves and cold spells.

Temperature extremes, heatwaves and cold spells occurrences have been calculated based in the dataset comprising daily interpolated maximum and minimum temperature observations from EDO for the

period 1981–2020 (Lavaysse et al., 2018). The temperature data is derived from an extensive network of approximately 4000 weather stations distributed across Europe and its adjacent regions. Interpolation of these temperature data was performed utilizing an inverse distance algorithm, with a search radius of 200 km and on a grid with a spatial resolution of 0.25 decimal degrees. A maximum of 20 nearby weather stations were considered for interpolation at any given location and a correction for elevation was applied by incorporating a temperature adjustment factor of 0.65 °C per 100 m of elevation change.

The definitions of heatwaves and cold spells, which are often subject to variability (Hong and Hong, 2016), were carefully chosen to align with widely accepted standards. For climatological heatwaves, the criteria set forth by the European Environment Agency (Crespi et al., 2020). A heatwave is defined thereby as a period of at least three consecutive days when the daily maximum temperature exceeds the 99th percentile of daily maximum temperature values from May to September in a given location over the reference climate period. Similarly, climatological cold spells have been defined as periods of at least three consecutive days when the daily minimum temperature is below the 1st percentile of daily minimum temperatures from November to March (Hooyberghs et al., 2019). In this context, the reference period for defining extreme temperature thresholds was established as 1981–2000.

2.10. Strong winds

Strong winds are defined as high-velocity air movements significantly exceeding typical or average wind speeds for a given region. In Europe, many of the most powerful windstorms originate in the North Atlantic Ocean during the winter session (Pryor et al., 2012). These storms are often referred to as North Atlantic storms or extratropical cyclones and can bring heavy rain and strong winds to western and northern Europe.

To assess the exposure of coastal cities to the forces of these winter storms, storm footprints were employed as a fundamental element. These footprints represent the spatial extent of each storm's impact. Specifically, for each storm track associated with windstorms occurring between October and March, the maximum 3 s 10 m wind gusts over a 72-h period were analysed for each coastal city. These data are sourced from ERA5 reanalysis and are based on hourly assessments, with a spatial resolution of 1.0 km (Copernicus Climate Change Service and Climate Data Store, 2022). To assess the potential hazard posed by these windstorms, a threshold was set at wind speeds exceeding 20 m/s, corresponding approximately to Beaufort Scale categories ranging from "gale" to "strong gale".

2.11. Landslides

Landslides can be defined as the abrupt downward movement of earth material, often triggered by various factors such as heavy rainfall, seismic activity, or human activities (Paranunzio et al., 2015). In this study, landslide exposure was assessed using data derived from the European Landslide Susceptibility v2 (ELSUS v2) dataset (Günther et al., 2014; Wilde et al., 2018). ELSUS v2 offers a comprehensive representation of landslide susceptibility across the European continent, characterized by a spatial resolution of 200 m. This dataset is the result of a heuristic-statistical modelling approach that integrates key landslide conditioning factors, encompassing slope angle, shallow sub-surface lithology, and land cover characteristics, in addition to geospatial information regarding over 149,000 actual landslide occurrences.

The resulting ELSUS v2 landslide susceptibility map classifies susceptibility levels into a categorical scale encompassing the following classifications: 'no data,' 'very low,' 'low,' 'moderate,' 'high,' and 'very high,' represented numerically within a range of 0–5. To evaluate the exposure of coastal cities to landslide susceptibility, an analysis focused on pixels corresponding to susceptibility levels of 4 and 5 was conducted for each coastal city domain. By aggregating these pixels, the corresponding area was computed and expressed as a percentage of the total land area occupied by each coastal city.

3. Results

Sea-level rise amplifies the adverse impacts of coastal flooding and erosion, progressively submerging land as mean sea level (MSL) continues to rise. A critical aspect of our analysis is the assessment of MSL rate variations for each coastal city. Our findings reveal a spectrum of MSL rates across these cities, ranging from 2.4 mm/year in Sligo to 5.4 mm/year in Vilanova i la Geltrú and Gdańsk. Intermediate MSL rates, falling between 3.4 mm/year and 3.8 mm/year, are observed in Benidorm, Massa, Piran, and Samsun. Dublin, Oarsoaldea, and Oeiras exhibit higher MSL rates, spanning from 4.0 mm/year to 4.5 mm/year (Fig. 1).

Considering the implications of these diverse MSL rates, it becomes evident that some coastal cities face a more rapid sea-level rise than others. This discrepancy underscores the need for tailored adaptation strategies and proactive measures in regions experiencing accelerated MSL increases. Moreover, understanding the underlying factors contributing to these disparities is crucial for informed decision-making and sustainable coastal management.

A comprehensive assessment that accounts for extreme high-tide, surge, and wave levels provides valuable insights into the potential for extreme sea level events in coastal cities. Fig. 2 presents an overview of the combined values of these crucial parameters. Notably, wave action emerges as the predominant contributor to the overall ESL across all coastal cities. The indicators show that Sligo, Oarsoaldea, and Oeiras are poised to experience the most substantial ESLs, reaching heights of 10.23 m, 8.07 m, and 7.61 m, respectively. Coastal cities situated along enclosed or semi-enclosed seas, such as the Mediterranean, Baltic, and Black Seas, generally exhibit lower ESL values, hovering around 3 m, with Samsun recording the lowest at 2.22 m. Tidal influence remains notably minimal in these cities, typically measuring less than 0.20 m, except for Piran, where it reaches 0.76 m. Surge levels exhibit variability among cities, with peak values observed in Sligo and Gdańsk at 1.12 m and 1.15 m, respectively.

These findings underscore the critical role of wave dynamics in shaping extreme sea levels in coastal cities, highlighting the significance of wave-related preparedness measures in these regions. Additionally, the notable differences in extreme sea levels among coastal cities, especially in relation to surge levels, raise questions about the local factors contributing to such variations. Further research into the specific geographic, geological, and environmental factors influencing surge levels in these regions could provide valuable insights for coastal planning and resilience efforts.

The quantification of coastal flooding extents and LECZ areas, as percentages of total city areas, provides a critical lens through which the vulnerability of European coastal cities to sea-level rise and potential inundation can be assessed. Fig. 2 juxtaposes these two pivotal indicators to identify areas most at risk of coastal flooding. The findings reveal a nuanced landscape of hazard across the studied cities. Specifically, the analysis based on the ECFAS dataset indicates that, with the exception of Oarsoaldea, coastal flooding extents are generally smaller than the corresponding LECZ areas. This discrepancy underscores the varied nature of threat landscapes, with Oarsoaldea presenting a unique case where the risk of coastal flooding aligns closely with its LECZ designation. In terms of relative coastal flooding exposure, Piran stands out, with 17.4% of its area falling within flood-prone zones, the highest among the cities studied, followed by Gdańsk with a notable 6.1% exposure.

Furthermore, Gdańsk emerges as the city with the highest LECZ proportion, with a staggering 46.8% of its total area falling within this zone. This finding underscores the acute vulnerability of Gdańsk to rising sea levels, demanding immediate attention to mitigate potential impacts on infrastructure, urban planning, and the livelihoods of its residents. Piran follows closely, with a substantial 29.1% of its city area

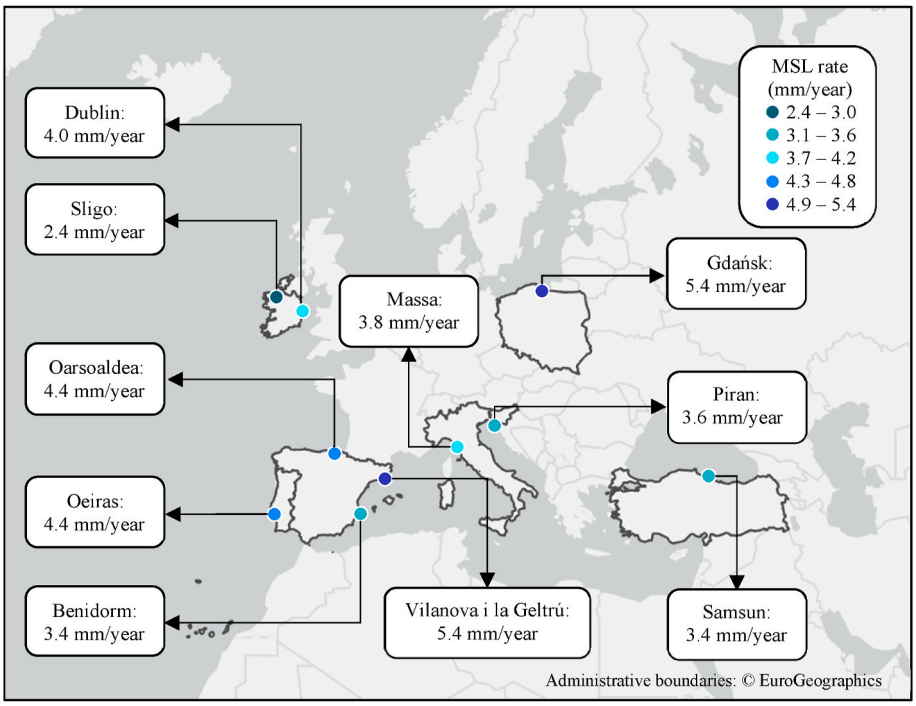

Fig. 1. Sea-level change rates in 2020 under the SSP2-4.5 scenario (relative to a 1995–2014 baseline). Data source: NASA Sea-Level Projection Tool (Garner et al., 2021; Intergovernmental Panel on Climate Change (IPCC), 2023; Kopp et al., 2023).

classified as LECZ. This places Piran in a high-risk category for coastal inundation, emphasizing the need for proactive measures to safeguard against sea-level rise-induced threats. Massa, with 18.6% of its area in the LECZ, also demonstrates a notable susceptibility to coastal hazards. The results suggest that Massa faces a considerable challenge in terms of preserving its coastal assets and managing potential flooding events. In contrast, cities such as Benidorm (3.0%), Oeiras (2.3%), and Oarsoaldea (1.1%) exhibit relatively lower LECZ proportions, indicating a comparatively reduced exposure to sea-level rise within their city boundaries. Dublin (15.6%), Samsun (9.6%), Sligo (8.3%) and Vilanova i la Geltrú (5.5%) fall within the medium range, indicating a need for comprehensive coastal management strategies to address potential impacts in these regions.

The indicators encompassing areas exposed to coastal flooding, defined as percentages of city territory, highlight the diverse range of coastal vulnerability levels across the studied cities. They underscore the critical importance of tailored adaptation and resilience strategies to safeguard these coastal regions and their communities from the escalating challenges posed by sea-level rise and coastal inundation.

The evaluation of coastal erosion, expressed as a percentage of the total city coastline, offers invaluable insights into the susceptibility of coastal cities to this widespread natural phenomenon (Fig. 3). It is worth noting that cities with artificial seafronts, where the impact of coastal erosion on these segments may be minimal, tend to exhibit lower susceptibility values. Additionally, it is important to acknowledge that some results may be outdated due to data being from 2004 or earlier, given the ongoing development of adaptation and mitigation efforts.

Massa presents a stark scenario, with its entire coastline affected by erosion, which translates into an alarming 100.0% susceptibility. This underscores the urgency of the extensive mitigation and adaptation actions undertaken in the region in recent years (Laino and Iglesias, 2023a). Piran (26.8%), Vilanova i la Geltrú (26.1%), Gdańsk (21.3%) and Sligo (19.6%) also have significant sections of coastline undergoing erosion. While not as severe as Massa, these cities nonetheless face significant challenges in managing and mitigating erosion impacts. Conversely, Dublin, Benidorm, and Oarsoaldea report 0.0% susceptibility, reflecting the presence of artificial seafronts or cliffs in these areas. However, it is essential to recognize that contemporary observations reveal ongoing coastal erosion affecting the Levante and Poniente beaches in Benidorm (Laino and Iglesias, 2023a; Toledo et al., 2022). Unfortunately, data for Samsun remained unavailable for this analysis. Nevertheless, other studies advocate for comprehensive data collection efforts to comprehensively assess and address this significant hazard in the coastal city (Faik and Sesli, 2010).

In summary, the assessment of coastline under erosion as a percentage of the total city coastline provides a crucial metric for understanding and comparing the vulnerability of coastal cities to this environmental challenge. These findings provide a solid foundation for targeted studies and the formulation of policy measures aimed at bolstering the resilience of these cities in the face of persistent coastal erosion.

The analysis of the extent of floods and water depths corresponding to river flooding events with a 100-year return period offers a critical perspective on the vulnerability of coastal cities to this specific hazard. As illustrated in Fig. 4, these data enables a comparative assessment of flood exposure across the study cities. It is important to note that the reference dataset does not encompass flooding events in areas with narrow (river width $<$100 m) watercourses or ravines, which may pose distinct flood risks. For such cases, we will delve into heavy rainfall events later in this study, providing additional insights into flood susceptibility.

In cities covered by the data from Dottori et al. (2021), flood extents and water depths have been combined (namely, LFI) to assess river flooding hazard. The LFI values are most pronounced in Gdańsk, Samsun, and Dublin, measuring at 55.72 cm, 20.75 cm, and 6.22 cm, respectively. This metric facilitates a direct comparison of river flood hazards among these cities. It is worth emphasizing that while the LFI cannot be accurately calculated for cities with small watercourses, our analysis highlights the historical prominence of river flooding hazards in Dublin, Gdańsk, and Samsun compared to the other cities under examination (Laino and Iglesias, 2023a). This underscores the continued relevance of the LFI as a valuable indicator for assessing and addressing river flood hazards.

The analysis of days with daily precipitation exceeding 20 mm

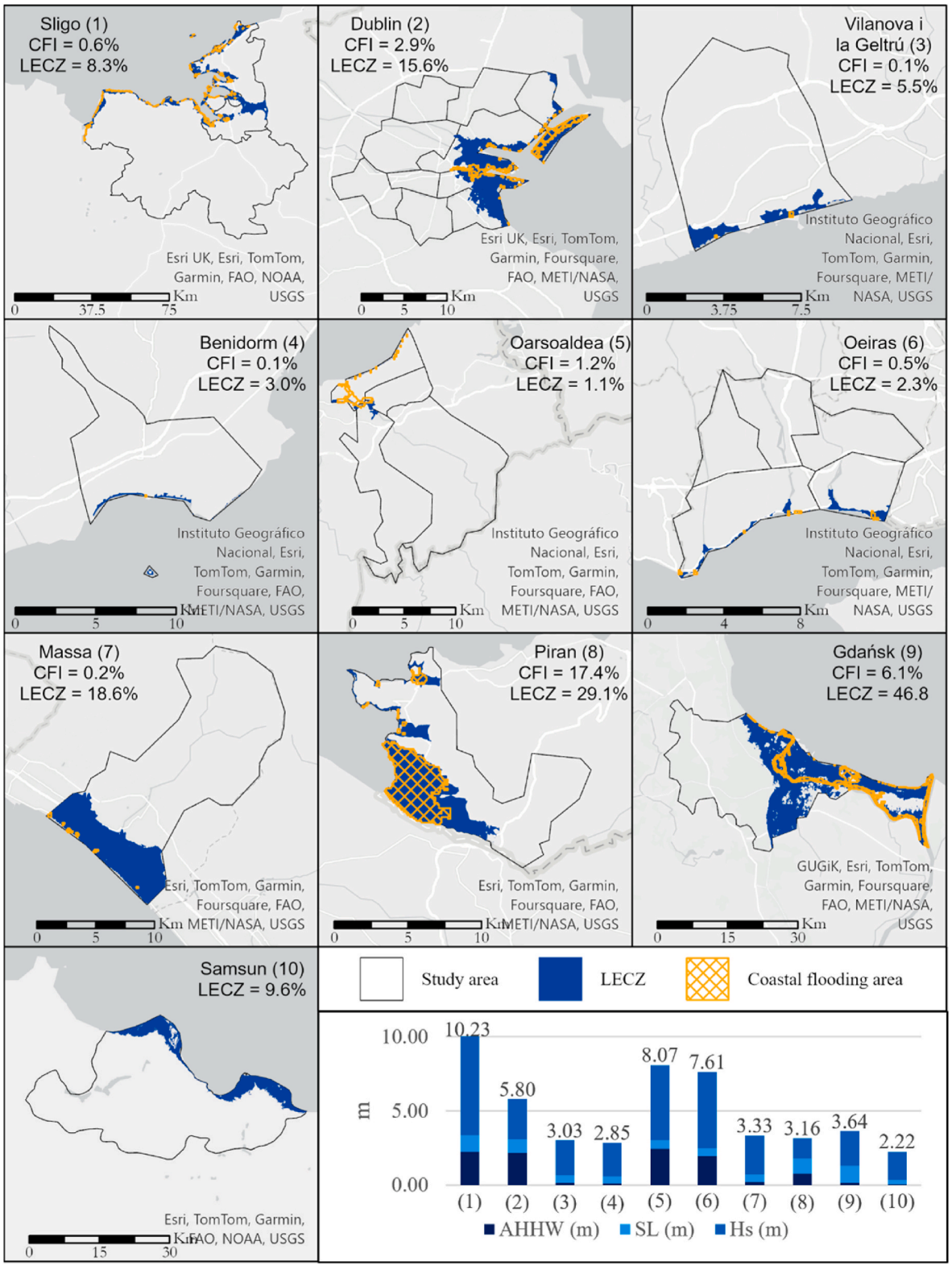

Fig. 2. Coastal flooding extents (CFI) based on the data from the ECFRAS Pan-EU Flood Catalogue for the synthetic storm scenario of 50-year return period and 36-h duration, LECZ extents and percentage expressing LECZ area over total city areas and averaged values of significant wave height (median of averaged 90th and 100th percentiles), surge (median of 50-year return period) and annual highest high water (median) levels between 2001 and 2017 for the coastal cities. Data source: Yamazaki et al. (2017) and ERA5 reanalysis (Caires and Yan, 2020; Hersbach et al., 2020; Yan et al., 2020).

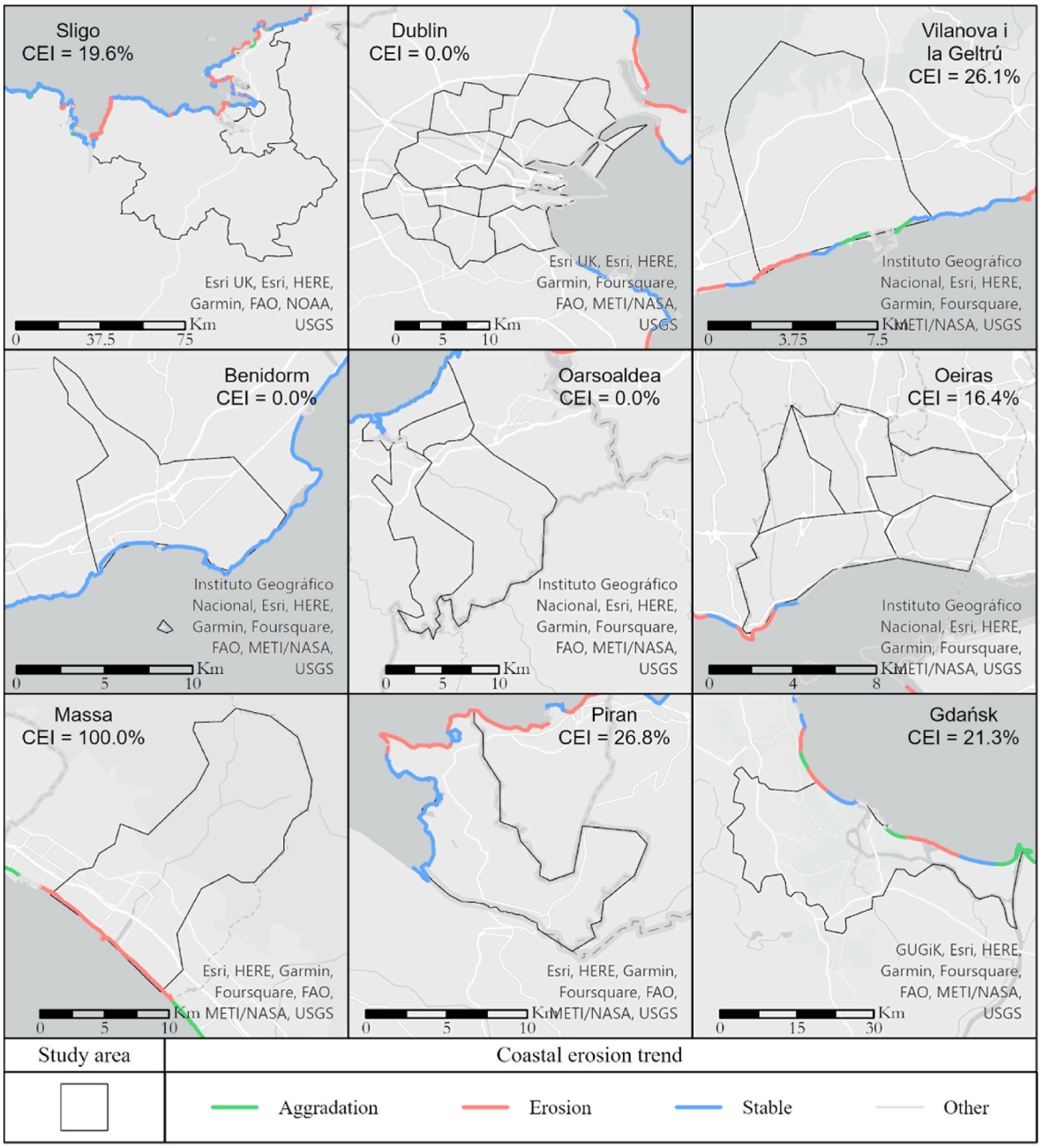

Fig. 3. Coastline evolution trends and percentage of coastline undergoing erosion over the total coastline length (CEI) for the coastal cities of Sligo, Dublin, Vilanova i la Geltrú, Benidorm, Oarsoaldea, Oeiras, Massa, Piran and Gdańsk. Data source: Eurosion (2004).

between 1981 and 2019 offers valuable insights into the susceptibility of coastal cities to heavy rainfall events (yearly averaged and scaled by a factor of 10^{-1} in Fig. 5 for visual comparison). This parameter displays noteworthy variations among the coastal cities under study. Massa, Piran, and Oarsoaldea stand out with the highest occurrences, tallying 821, 685, and 546 instances, respectively. In contrast, Gdańsk, Benidorm, and Dublin record the lowest occurrences, with 52, 106, and 109 instances, respectively. Meanwhile, Sligo, Vilanova i la Geltrú, Oeiras, and Samsun accumulate around 200 days of such heavy rainfall events, with 244, 228, 170, and 198 occurrences, respectively. Significant trend changes are not apparent across the coastal cities between 1981-2000 and 2001–2019. However, there is a subtle increase in the number of heavy rainfall events observed in Dublin and Benidorm during this period.

These findings underscore the diversity in heavy rainfall exposure among coastal cities, with some cities consistently experiencing a higher frequency of such events. While overall trends remain relatively stable, the slight uptick in heavy rainfall events in Dublin and Benidorm suggests the need for continued monitoring and adaptation strategies to address potential increases in extreme precipitation in these regions. However, it is worth noting that while this study provides valuable insights into the frequency of heavy rainfall events in coastal cities, changes in rainfall intensity have not been examined specifically. Future research should delve deeper into the intensity of precipitation events, as this aspect can provide a more comprehensive understanding of the evolving precipitation patterns and their potential impacts on these coastal regions (Skougaard Kaspersen et al., 2017).

The examination of the number of months with SPI-03 below −1 (1981–2020) as depicted in Fig. 5 serves as a valuable indicator of the likelihood of drought episodes in coastal cities. Oeiras stands out with

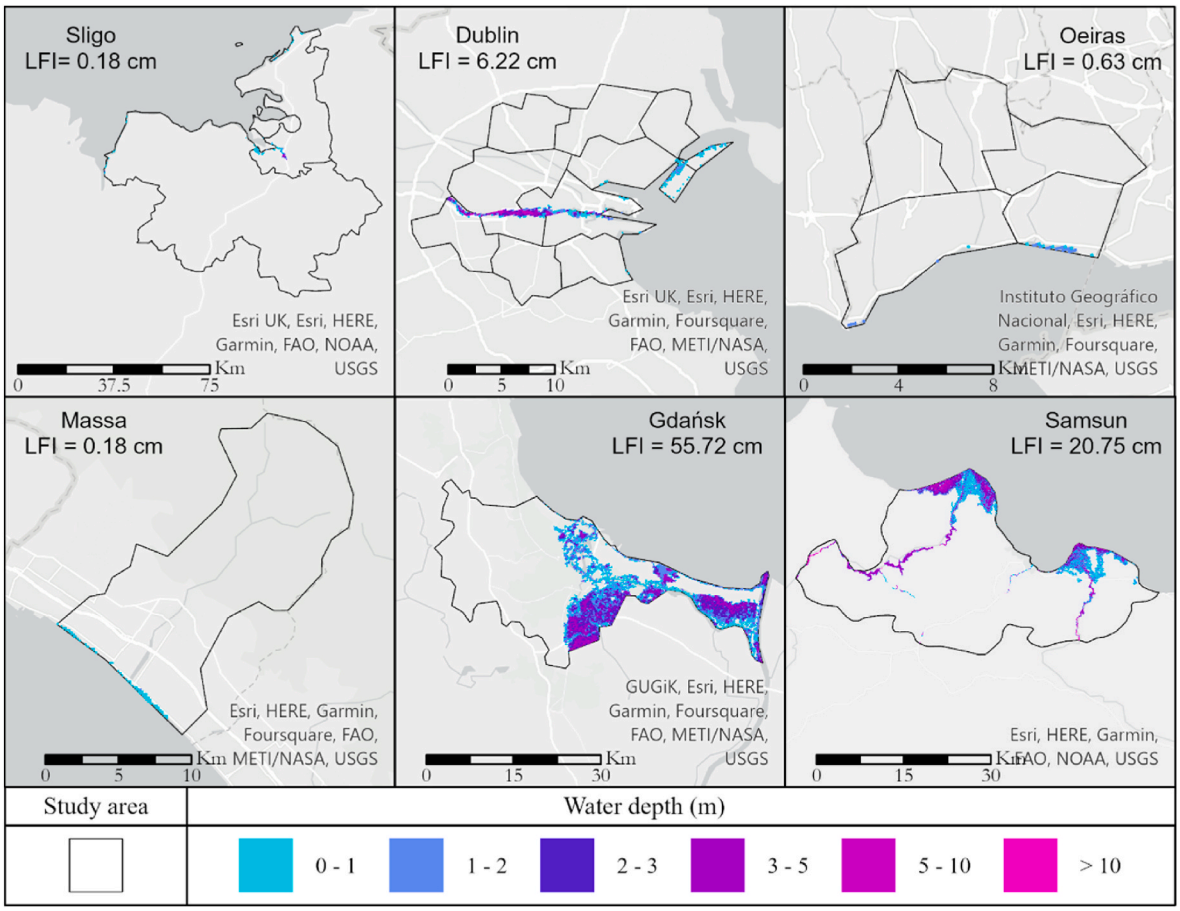

Fig. 4. Water depths and height (cm) corresponding to the elevation of the flood volume relative to the total area of each coastal city (LFI) for river flooding events of 100-year return period. Cities where flood extents are null are not represented. Data source: Dottori et al. (2021).

the highest cumulative count of such months, registering at 91 (Espinosa and Portela, 2022; Santos et al., 2010). Notably, these drought events have become more prevalent in the past two decades, increasing from 38 months (1981–2000) to 53 months (2001–2020). Sligo and Piran also exhibit substantial counts, with 82 and 85 months respectively falling under these defined drought conditions during the period of 1981–2020. Similar to Oeiras, Sligo and Piran have witnessed an escalation in drought events, with 33 months–49 months and 32 months–53 months respectively, when comparing the time spans of 1981–2000 and 2001–2020.

Conversely, coastal cities such as Dublin (61), Benidorm (63), and Gdańsk (64) record lower total counts of drought months for the same period. In some of these cities, namely Benidorm (42 against 21), Gdańsk (38 against 26), and Samsun (41 against 35), there is even a declining trend in drought months, suggesting a relative mitigation of drought risk in recent years. Additionally, several coastal cities, including Vilanova i la Geltrú (78), Oarsoaldea (74), Massa (73), and Samsun (76), exhibit intermediate total counts of drought months. Notably, Massa demonstrates a significant increase in drought months between 1981-2000 and 2001–2020, rising from 29 to 44 months.

These findings emphasize the need for proactive drought management strategies in cities with increasing drought trends, while also highlighting the decrease of drought-risk in others. Tailored approaches to drought resilience should take into account the specific challenges faced by each coastal city, as demonstrated by the variations in drought occurrence and trends across the studied regions.

The calculation of extreme temperature values based on daily minimum and maximum temperature data yields a wealth of critical information. Beyond facilitating the assessment of heatwaves and cold spells, which will be discussed in detail later, these indicators offer invaluable insights with wide-ranging applications, encompassing climate resilience planning, public health, infrastructure development, energy management, agricultural practices, tourism, climate mitigation strategies, and emergency preparedness, among others.

Table 3 illustrates the 99th percentile for daily maximum temperatures and the 1st percentile for daily minimum temperatures between 1981 and 2000 across the coastal cities in our study. Notably, Oeiras stands out as the coastal city with the highest recorded maximum temperature, reaching a scorching 38.2 °C. It is closely followed by Oarsoaldea, Vilanova i la Geltrú, and Benidorm, all located in the Iberian Peninsula, with maximum temperatures of 35.2 °C, 34.4 °C and 34.4 °C, respectively. Conversely, Gdańsk emerges as the coastal city with the most frigid recorded minimum temperature, plummeting to −16.3 °C. This stark contrast is followed by Massa (−6.4 °C), Samsun (−5.9 °C), and Sligo (−5.7 °C), emphasizing the considerable variation in minimum temperature extremes among the studied coastal cities. Notably, Dublin and Sligo, both situated in Ireland, exhibit the lowest recorded high temperatures among the coastal cities, with values of 24.5 °C and 24.3 °C, respectively. Regarding the maximum recorded low temperatures, the Iberian Peninsula cities once again lead the pack, with Oeiras and Vilanova i la Geltrú registering 2.8 °C, Benidorm recording −1.8 °C, and Oarsoaldea reporting −3.2 °C.

These temperature extremes underscore the vast climatic diversity across the coastal cities under study, with some experiencing sweltering high temperatures while others endure extreme cold. The comprehensive nature of this temperature analysis not only aids in understanding local climate patterns but also highlights the multifaceted implications for various sectors and industries operating in these regions.

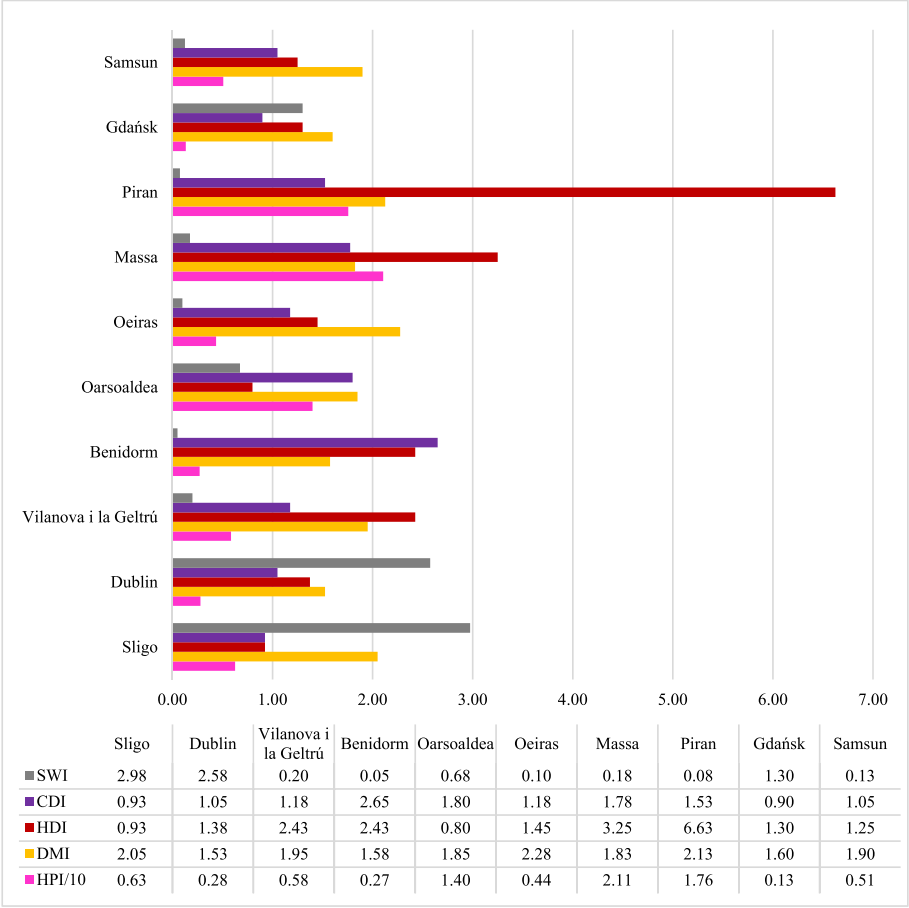

	Sligo	Dublin	Vilanova i la Geltrú	Benidorm	Oarsoaldea	Oeiras	Massa	Piran	Gdańsk	Samsun
SWI	2.98	2.58	0.20	0.05	0.68	0.10	0.18	0.08	1.30	0.13
CDI	0.93	1.05	1.18	2.65	1.80	1.18	1.78	1.53	0.90	1.05
HDI	0.93	1.38	2.43	2.43	0.80	1.45	3.25	6.63	1.30	1.25
DMI	2.05	1.53	1.95	1.58	1.85	2.28	1.83	2.13	1.60	1.90
HPI/10	0.63	0.28	0.58	0.27	1.40	0.44	2.11	1.76	0.13	0.51

Fig. 5. Yearly-averages of number of days with daily precipitation exceeding 20 mm (HPI) (1981–2019), number of months with SPI-03 below −1 (DMI) (1981–2020), heatwave days (HDI) (1981–2020), cold spell days (CDI) (1981–2000) and number of windstorms events with maximum 3 s and 10 m height wind gust velocities exceeding 20 m/s (SWI) (1981–2020). Data source: Mercogliano et al. (2021), European Commission and Joint Research Centre (JRC) (2021), Lavaysse et al. (2018) and Copernicus Climate Change Service, Climate Data Store (2022).

Table 3
Percentiles 99th for daily maximum temperatures and 1st for daily minimum temperatures between 1981 and 2000 for the coastal cities. Data source: (Lavaysse et al., 2018).

Coastal city	Low extreme temperature threshold (°C)	High extreme temperature threshold (°C)
Sligo	−5.7	24.3
Dublin	−4.5	24.5
Vilanova i la Geltrú	2.8	34.4
Benidorm	−1.8	34.4
Oarsoaldea	−3.2	35.2
Oeiras	2.8	38.2
Massa	−6.4	30.6
Piran	−4.1	32.9
Gdańsk	−16.3	29.8
Samsun	−5.9	33.9

The analysis of heatwaves and cold spells in this study focuses on instances when daily maximum temperatures, in the case of heatwaves, and daily minimum temperatures, in the case of cold spells, surpass predefined thresholds based on percentiles. Periods lasting three or more days with these conditions occurring between 1981 and 2020 were evaluated for the coastal cities, with the yearly-averaged cumulative duration of these events presented in Fig. 5.

In the context of heatwaves, Piran emerges as a standout, with a total duration of 265 days of heatwave conditions recorded over the four decades under scrutiny. Massa follows in second place with 130 days, while Benidorm and Oarsoaldea rank third, each experiencing 97 days of heatwave conditions. Conversely, Gdańsk, Samsun, Sligo, and Oarsoaldea report the lowest duration of heatwave events, with 52, 50, 37, and 32 days, respectively. When examining cold spells, the variation in duration between the first and second places is less pronounced. Benidorm leads with 106 cumulative days of cold spells, followed closely by Oarsoaldea with 72 days. Massa ranks third with 71 days, while Piran records 61 days. Gdańsk, Sligo, Dublin, and Samsun occupy the lower positions in terms of cold spell duration, with 36, 37, 42, and 42 days, respectively. Interestingly, it is evident that the frequency of heatwaves and cold spells doesn't necessarily correlate directly with the extremity of temperature values in general. For example, Gdańsk, known for having the coldest recorded minimum low temperature, reports a relatively lower frequency of cold spells. Moreover, coastal cities such as Sligo, Dublin, Oeiras, Gdańsk, and Samsun experience lower frequencies of both heatwaves and cold spells. In contrast, Benidorm, Massa, and Piran exhibit relatively higher frequencies of these events.

These findings emphasize that the occurrence and duration of heatwaves and cold spells are influenced by a complex interplay of local climate factors, and they do not necessarily align with the extremity of temperature values alone. These phenomena not only impact the local environment but also have significant implications for the residents and various sectors operating within these cities. For instance, cities with higher occurrences of heatwaves may need to prioritize public health measures, such as heat action plans, to protect vulnerable populations during extended periods of extreme heat. Conversely, regions experiencing frequent cold spells may require infrastructure and energy

management strategies to ensure resilience in the face of cold-related disruptions. Furthermore, it is essential to recognize that these variations in temperature extremes can influence urban planning, tourism trends, and even agricultural practices. By understanding the intricacies of heatwaves and cold spells within the context of specific coastal cities, policymakers and stakeholders can make more informed decisions to enhance climate adaptation and improve the overall quality of life for their communities.

Remarkably, Sligo and Dublin, both located in Ireland, emerge as the most exposed to these intense wind events, with a cumulative count of 119 and 103 strong wind occurrences, respectively (Fig. 5). These figures underscore the vulnerability of these regions to the fierce winter storms that sweep across the Atlantic Ocean. Such exposure can pose significant challenges, including infrastructure damage, power outages, and coastal erosion, necessitating robust resilience planning and preparedness measures. Conversely, Gdańsk and Oarsoaldea record comparatively lower counts of 52 and 27 strong wind events, indicating a relatively reduced exposure to extreme wind conditions during the winter season. While these cities are not immune to the impacts of winter storms, their lower exposure levels may mitigate some of the associated risks. The remaining coastal cities in our study report occurrences of less than 10, underscoring their comparatively lower susceptibility to such potent wind gusts. This variance in exposure highlights the diverse range of challenges faced by coastal communities in Europe.

Sligo and Dublin, positioned along the Atlantic coast, consistently experience a higher frequency of these events, potentially reflecting the influence of Atlantic winter storms. This correlation invites further

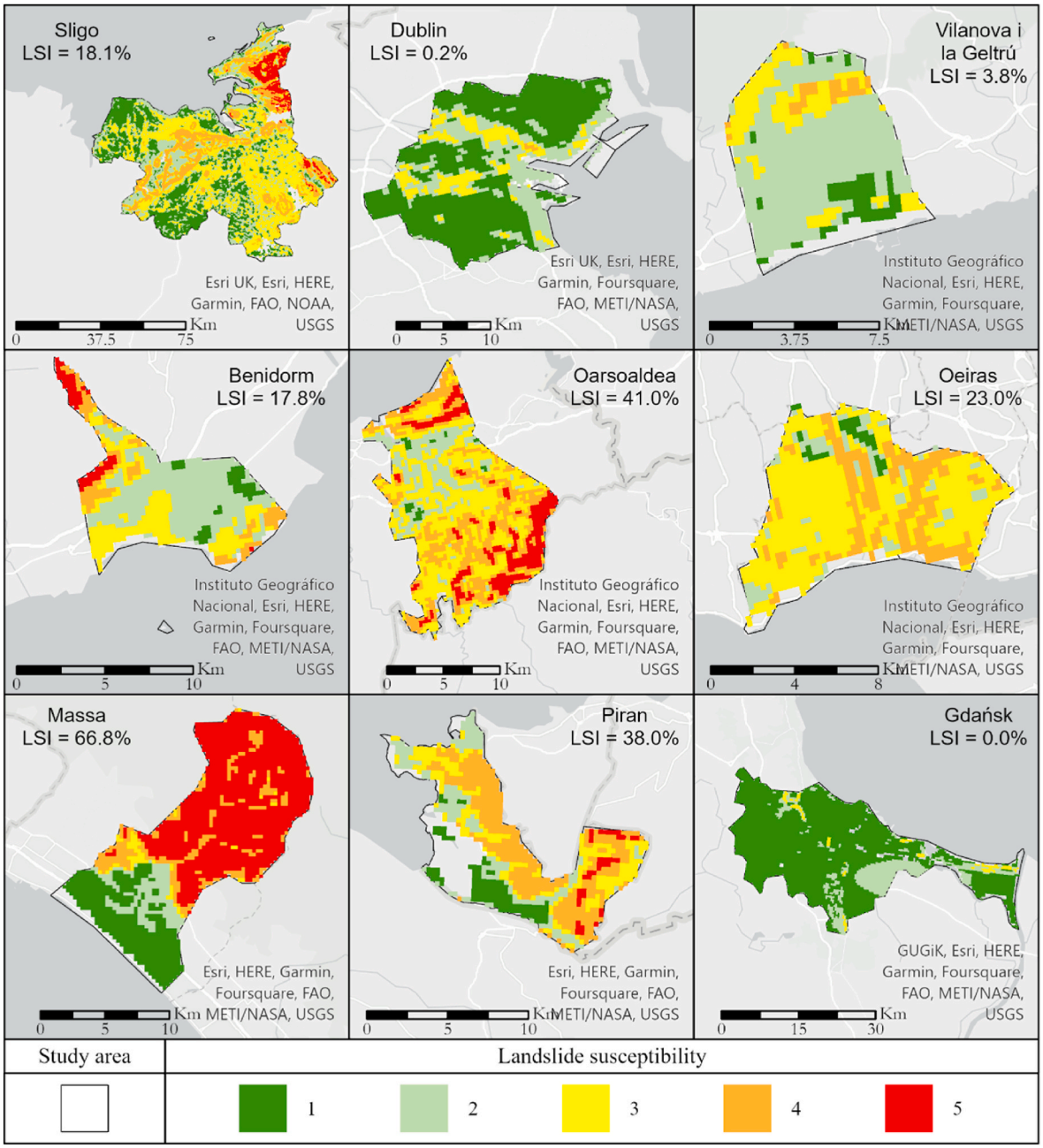

Fig. 6. Landslide susceptibility indicator (LSI) measured as the percentage of the area corresponding to the landslide susceptibility levels 4 (high) and 5 (very high) over the total area for the coastal cities of Sligo, Dublin, Vilanova i la Geltrú, Benidorm, Oarsoaldea, Oeiras, Massa, Piran and Gdańsk. Data source: Günther et al. (2014) and Wilde et al. (2018).

investigation into the specific meteorological patterns that shape the exposure of coastal cities to extreme winter winds, offering valuable insights for climate resilience and risk mitigation strategies.

The calculation of susceptibility levels 4 (high) and 5 (very high) for each coastal city, except for Samsun due to data limitations, provides valuable insights into the potential landslide hazards faced by these regions. When expressed as a fraction of the total city area (Fig. 6), this indicator reveals a wide spectrum of susceptibility levels, ranging from 0.0% in Gdańsk to a significant 66.8% in Massa. Remarkably, Massa stands out with the highest susceptibility level, covering almost two-thirds of its city area (66.8%), emphasizing the heightened landslide risk in this region. Oarsoaldea (41.0%) and Piran (38.0%) also record substantial values, underscoring the importance of landslide mitigation efforts in these areas. In contrast, Oeiras (23.0%), Benidorm (17.8%), and Sligo (18.1%) exhibit medium levels of susceptibility, indicating a moderate but notable vulnerability to landslide hazards. These cities would benefit from targeted measures to enhance their resilience against potential landslide events. Conversely, Vilanova i la Geltrú (3.2%), Dublin (0.2%), and Gdańsk (0.0%) report the lowest susceptibility values, suggesting a relatively lower risk of landslides in these coastal cities.

The varying degrees of landslide susceptibility among coastal cities underscore the need for region-specific strategies to address this hazard effectively. Cities with high susceptibility, such as Massa, may require extensive measures to mitigate landslide risks and protect vulnerable areas. Meanwhile, cities with medium susceptibility levels, like Oeiras, Benidorm, and Sligo, should prioritize adaptive measures that balance the potential risks and resources available. Lastly, cities with low susceptibility levels, including Vilanova i la Geltrú, Dublin, and Gdańsk, may still benefit from proactive planning and monitoring to ensure long-term resilience.

4. Discussion

The integrated approach developed in this work provides valuable insights into the multifaceted challenges faced by coastal cities in relation to climate-related hazards, ensuring that adaptation and resilience strategies are not developed in isolation but are informed by a comprehensive understanding of the local context (Tiwari et al., 2022). The high-level characterisation of coastal hazards integrates a combination of indicators, including sea-level rise rates, extreme sea levels, coastal erosion susceptibility, coastal flooding extents, and LECZ areas. These results underscore the extent to which coastal cities are exposed to sea-level rise and the potential for inundation and coastal erosion. The comparison of the results between the coastal cities emphasizes the acute exposure of some cities to these hazards, highlighting the urgent need for proactive measures. Piran and Gdansk present the worst scenarios regarding areas exposed to coastal hazards, whereas the cities situated along the Atlantic Ocean face higher water levels, which is coherent with existing studies (Brečko Grubar et al., 2019; Lin-Ye et al., 2020; Paprotny and Terefenko, 2017; Paranunzio et al., 2022). However, it is essential to emphasize that even in cities with lower exposure, the potential impact of sea-level rise should not be underestimated, warranting continuous monitoring and adaptive planning (Irene et al., 2010).

Nonetheless, the selection of optimal return periods and percentiles for the previous indicators is a pivotal consideration for further analyses (Tu et al., 2017). Generally, shorter return periods, such as 2, 5, or 10 years, serve to evaluate the city's susceptibility to more frequent yet less severe surge events, making them instrumental in assessing vulnerabilities in infrastructure and property for common coastal flooding occurrences. Conversely, longer return periods, such as 25, 50, or 100 years, are employed to address less frequent but more intense surge events, playing a pivotal role in the design and fortification of critical infrastructure against rare, high-impact events. The selection of the most suitable return period should be underpinned by an intricate evaluation of factors including risk tolerance, financial constraints, and the criticality of assets and human populations exposed to the ESLs (Keighley et al., 2018). For instance, a comprehensive risk assessment necessitates the consideration of multiple return periods to encapsulate the spectrum of plausible ESL scenarios.

This work recognises the role of indicators that may appear non-correlated or less directly relevant to coastal hazards yet significantly influence policy-making processes. The developed indicators include broader climate-related hazards not exclusive to coastal contexts, namely heavy rainfall, land flooding, droughts, extreme temperatures, heatwaves, cold spells, landslides, and strong winds. As these hazards also affect urban resilience, infrastructure vulnerability, and community preparedness, the approach enables well-rounded policy responses, by covering a diverse spectrum of climate-related hazards inherent in urban coastal environments (Paranunzio et al., 2024).

In cities covered by the data, flood extents and water depths have been combined to assess river flooding hazard. While it is important to note that this reference dataset does not encompass flooding events in areas with narrow watercourses or ravines (Laino and Iglesias, 2023c), i.e., Benidorm (Sánchez-Almodóvar et al., 2023), the findings are still illuminating. These values facilitate a direct comparison of river flood hazards among these cities, highlighting the historical prominence of river flooding hazards in Dublin, Gdańsk, and Samsun (Demir and Kisi, 2016; Marosz, 2007; Paranunzio et al., 2022). This underscores the continued relevance of this indicator for assessing and addressing river flood hazards.

The analysis of days with daily precipitation exceeding 20 mm between 1981 and 2019 offers valuable insights into the susceptibility of coastal cities to heavy rainfall events. Some cities, such as Massa, Piran, and Oarsoaldea, experience a higher frequency of these events, while others like Gdańsk, Benidorm, and Dublin record lower occurrences (D'Amato Avanzi et al., 2013; Rivas et al., 2020; Sacchi, 2012). While overall trends remain relatively stable, the slight uptick in heavy rainfall events in Dublin and Benidorm suggests the need for continued monitoring and adaptation strategies to address potential increases in extreme precipitation in these regions (Martínez-Ibarra, 2015). It is important to note that these findings emphasize the diversity in heavy rainfall exposure among coastal cities. Researchers may also want to examine factors like the intensity, duration, and spatial extent of heavy rainfall events to gain a more comprehensive understanding (Espinosa et al., 2022; Ishida et al., 2018).

In our approach, the SPI-3 values enabled us to discern periods of below-average precipitation, subsequently identifying and tallying the months characterized by meteorological drought conditions for each city (Trinh et al., 2017). Coastal cities like Oeiras, Sligo, and Piran exhibit substantial counts of months falling under these defined drought conditions (Cunha et al., 2018; Santos et al., 2010). While some cities experience an increase in drought events, others, like Benidorm, Gdańsk, and Samsun, report lower counts and even a decline in drought months. These findings emphasize the need for proactive drought management strategies in cities with increasing drought trends, while also highlighting the decrease of drought risk in others. While the SPI-3 with a threshold of -1 is a widely accepted criterion, it is important to note that the choice of threshold can influence the identification of drought events. The appropriateness of this indicator may vary depending on the specific research objectives and the regional climatic characteristics of the study area (Liu et al., 2019). Therefore, its usage in this study was contingent upon its applicability to the context of the investigation and the availability of relevant data. Additionally, the spatial resolution of 1° in the SPI-3 data may smooth out local variations in drought conditions. These limitations should be considered when interpreting the results.

The measurement of extreme temperatures using relative thresholds from daily minimum and maximum temperature values permits the assessment and comparison of changes in unusually warm or cold days at different locations, independently of the baseline climate. These

thresholds take into account the local climate and variations, making them a valuable tool for assessing climate-related risks and vulnerabilities. Results highlight the climatic diversity across the coastal cities (from the highest maximum temperature of 38.2 °C in Oeiras to the coldest minimum temperature of −16.3 °C in Gdańsk) (Dessai, 2003). Similarly, the analysis of heatwaves and cold spells in this study focuses on instances when daily maximum and minimum temperatures surpass these relative thresholds. Some cities, like Piran and Massa, experience a high duration of heatwave conditions, while others, such as Gdańsk and Sligo, record lower occurrences. Results show that the frequency and duration of heatwaves and cold spells are influenced by complex local climate factors, and they do not necessarily correlate directly with the extremity of temperature values alone.

In assessing landslide hazards among diverse coastal cities, the application of susceptibility levels 4 (high) and 5 (very high) as a relative fraction of total city area serves as a practical and informative tool for comparison. By quantifying the proportion of city area with higher susceptibility, we can readily identify regions most exposed, such as Massa and Oarsoaldea (D'Amato Avanzi et al., 2013; Nardi and Rinaldi, 2015; Rivas et al., 2020). Other cities exhibit varying degrees of landslide susceptibility, emphasizing the need for region-specific strategies to address this hazard effectively. This comparative approach aids in prioritizing resources, targeting mitigation efforts, and guiding policy decisions tailored to the specific landslide risk profiles of each coastal city.

The determination of the frequency and spatial distribution of wind events exceeding the defined threshold in close proximity to the selected coastal cities facilitated a high-level evaluation of their exposure to strong winds during the winter season. Sligo and Dublin, situated along the Atlantic coast, experience a notably higher frequency of strong wind events, potentially reflecting the influence of Atlantic winter storms. This correlation invites further investigation into the specific meteorological patterns that shape the exposure of coastal cities to extreme winter winds, offering valuable insights for climate resilience and risk mitigation strategies.

The importance of differentiating between densely built and non-built coastal zones is recognized, as urban density significantly influences the vulnerability and potential impacts of coastal hazards. The selection of cities within this study was designed to encompass a broad spectrum of urban settings, ranging from densely populated metropolitan areas to less developed coastal regions. This strategy ensures the applicability of the findings across diverse urban contexts, offering insights into the general exposure to coastal hazards. However, it is acknowledged that the methodology primarily focuses on the delineation and analysis of physical climate-related hazards. While urban density and land use patterns are crucial for a comprehensive understanding of vulnerability and exposure to these hazards, such indicators were not the central focus of this research. The emphasis was placed on establishing a baseline understanding of hazard prevalence and intensity, crucial for initiating the broader process of risk assessment. Future research is suggested to expand on the findings by incorporating detailed assessments of vulnerability and exposure. These should include considerations of urban density, infrastructure resilience, population dynamics, and socio-economic factors to provide a holistic risk profile for coastal cities. By concentrating on hazard identification and characterization, this study contributes to the foundational knowledge required for more detailed analyses of vulnerability and exposure. It lays the groundwork for subsequent research to integrate urban density considerations, among other factors, thereby enhancing strategies for risk reduction and resilience improvement in coastal urban environments.

5. Conclusions

The indicator-based approach devised in this work enables multiple climate-related hazards to be compared in ten European coastal cities in a systematic, standardized manner. The comparison and contrast of the findings from different types of coastal cities allows for the identification of commonalities and differences, recognition of patterns, and development of a more comprehensive understanding of climate-related hazards on regional or national scales. Leveraging the influence of climate-related hazards enables policymakers, urban planners, and communities to make well-informed decisions regarding urban planning, land-use management, infrastructure development, adaptation strategies and disaster risk reduction (Ouyang et al., 2016).

The methodology presented herein is founded on a series of hypotheses tailored to the unique challenges that coastal cities face in relation to climate-related hazards. First, the coastal cities are collectively and systematically examined, enabling decision-making bodies to discern varying climate-related hazards and prioritize budget allocation based on the degree of exposure. By applying this methodology, decision-makers can efficiently identify the specific needs of each coastal city and allocate resources more effectively to mitigate potential hazards. This hypothesis implies that the methodology encompasses various coastal cities concurrently. Conversely, the methodology is not devised to evaluate the coastal cities in isolation; rather, its purpose is to compare climate-related hazards among them. Consequently, this approach is not aimed at detailed local studies.

Second, the methodology concentrates on the coastal cities themselves. Numerous indicator-based approaches have been developed to appraise extensive coastal regions, rather than specifically focusing on coastal cities. The methodology described in this work is explicitly devised for assessing coastal cities and their associated coastal areas. This methodology permits the incorporation of specific aspects unique to the coastal cities, which might otherwise be disregarded. These aspects include the different characteristics of the cities (size, morphology, population, urbanization, ecosystems, etc.), current state of the related literature, involvement of local expertise, identification of key climate-related hazards and consideration of local coastal adaptation planning, among others.

Third, the methodology is suitable for evaluating multiple climate-related hazards. This suitability arises from the fact that the coastal cities encompass diverse climatic regions, resulting in variations in climate-related hazards among them. Consequently, the proposed set of indicators captures essential aspects related to hazard exposure for each selected coastal city and climate-related hazard. These indicators are meticulously designed to be applicable elsewhere, allowing for standardized comparisons across different geographical contexts.

Fourth, the availability of data is very heterogeneous between the coastal cities. In certain instances, global datasets have been utilized to construct these indicators. However, it should be noted that the spatial resolution and uncertainty of the global datasets may be insufficient for the study areas with limited geographical coverage, such as Vilanova i la Geltrú, Benidorm, and Massa.

Fifth, the methodology allows for refinement. In this process, a set of indicators is employed to evaluate the different coastal cities collectively. In future stages, the weights assigned to these indicators may be adjusted by each coastal city according to their individual criteria, or even new indicators may be introduced. Furthermore, if higher-resolution datasets become available, the indicators can be assessed with increased precision. Consequently, the methodology can be continuously improved, while the level of detail can be increased.

Finally, it is crucial to recognize that the evaluation is characterized by a high-level approach based on indicators. Conducting a thorough evaluation of each city would necessitate an exhaustive study incorporating localized data, climate models, and assessments by local authorities (Tansel, 1995). The information provided herein serves as a general basis for comparison. Notwithstanding, the application of the proposed methodology can serve as a basis for further quantitative assessments.

CRediT authorship contribution statement

Emilio Laino: Writing – review & editing, Writing – original draft, Software, Methodology, Investigation, Formal analysis, Data curation, Conceptualization. **Gregorio Iglesias:** Writing – review & editing, Writing – original draft, Supervision, Project administration, Funding acquisition, Conceptualization.

Declaration of competing interest

The authors declare that they have no known competing financial interests or personal relationships that could have appeared to influence the work reported in this paper.

Data availability

The authors do not have permission to share data.

Acknowledgements

E. Laino acknowledges the support of the European Commission through the SCORE project, SMART CONTROL OF THE CLIMATE RESILIENCE IN EUROPEAN COASTAL CITIES, H2020-LC-CLA-13-2020, Project ID: 101003534. The authors are grateful to the SCORE consortium and, in particular, the Coastal City Living Labs for the valuable local knowledge.

We thank the projection authors for developing and making the sea-level rise projections available, multiple funding agencies for supporting the development of the projections, and the NASA Sea-Level Change Team for developing and hosting the IPCC AR6 Sea-Level Projection Tool.

We acknowledge the E-OBS dataset from the EU-FP6 project UERRA (https://www.uerra.eu) and the Copernicus Climate Change Service, and the data providers in the ECA&D project (https://www.ecad.eu).

Caires and Yan (2020), Hooyberghs et al. (2019), Mercogliano et al. (2021) and Yan et al. (2020) were downloaded from the Copernicus Climate Change Service (C3S) (2023).

The results contain modified Copernicus Climate Change Service information 2023. Neither the European Commission nor ECMWF is responsible for any use that may be made of the Copernicus information or data it contains.

References

Ahsan, MdN., Warner, J., 2014. The socioeconomic vulnerability index: a pragmatic approach for assessing climate change led risks–A case study in the south-western coastal Bangladesh. Int. J. Disaster Risk Reduc. 8, 32–49. https://doi.org/10.1016/j.ijdrr.2013.12.009.

Antunes, C., Rocha, C., Catita, C., 2019. Coastal flood assessment due to Sea Level rise and extreme storm events: a case study of the atlantic coast of Portugal's mainland. Geosciences. https://doi.org/10.3390/geosciences9050239.

Baccini, M., Kosatsky, T., Analitis, A., Anderson, H.R., D'Ovidio, M., Menne, B., Michelozzi, P., Biggeri, A., 2009. Impact of heat on mortality in 15 European cities: attributable deaths under different weather scenarios. J. Epidemiol. Community Health 65, 64–70. https://doi.org/10.1136/jech.2008.085639, 1978.

Barredo, J.I., 2007. Major flood disasters in Europe: 1950–2005. Nat. Hazards 42, 125–148. https://doi.org/10.1007/s11069-006-9065-2.

Beden, N., Ulke, A., 2020. Flood hazard assessment of a flood-prone intensively urbanized area -A case study from Samsun Province, Turkey. Geofizika 37, 2020. https://doi.org/10.15233/gfz.2020.37.2.

Bergillos, R.J., Rodriguez-Delgado, C., Medina, L., Iglesias, G., 2020a. Coastal cliff exposure and management. Ocean Coast Manag. 198, 105387 https://doi.org/10.1016/j.ocecoaman.2020.105387.

Birkmann, J., Dech, S.W., Hirzinger, G., Klein, R., Klüpfel, H., Lehmann, F., Mott, C., Nagel, K., Schlurmann, T., Setiadi, N.J., Siegert, F., Strunz, G., 2006. Measuring Vulnerability to Promote Disaster-Resilient Societies: Conceptual Frameworks and Definitions.

Brečko Grubar, V., Kovačic, G., Kolega, N., 2019. Climate change increasing frequency of sea flooding. Geogr. V. Soli 27, 30–34.

Buriks, C., Bohn, W., Kennett, M., Scola, L., Srdanovic, B., 2004. Using HAZUS-MH for Risk Assessment: How-To Guide.

Cai, Y.P., Huang, G.H., Tan, Q., Chen, B., 2011. Identification of optimal strategies for improving eco-resilience to floods in ecologically vulnerable regions of a wetland. Ecol. Model. 222, 360–369. https://doi.org/10.1016/j.ecolmodel.2009.12.012.

Caires, S., Yan, K., 2020. Ocean surface wave indicators for the European coast from 1977 to 2100 derived from climate projections. Copernicus Climate Change Service (C3S) Climate Data Store (CDS). https://doi.org/10.24381/cds.1a072dd6 [WWW Document].

Chen, S., He, Y., Tan, Q., Hu, K., Zhang, T., Zhang, S., 2022. Comprehensive assessment of water environmental carrying capacity for sustainable watershed development. J. Environ. Manag. 303, 114065 https://doi.org/10.1016/j.jenvman.2021.114065.

Copernicus Climate Change Service, Climate Data Store, 2022. Winter windstorm indicators for Europe from 1979 to 2021 derived from reanalysis. Copernicus Climate Change Service (C3S) Climate Data Store (CDS). https://doi.org/10.24381/cds.9b4ea013 [WWW Document].

Crespi, A., Terzi, S., Cocuccioni, S., Zebisch, M., Berckmans, J., Füssel, H.-M., 2020. "Climate-related hazard indices for Europe". European topic Centre on climate change impacts. Vulnerability and Adaptation (ETC/CCA) Technical Paper 2020/1. https://doi.org/10.25424/cmcc/climate_related_hazard_indices_europe_2020.

Cunha, L., Dimuccio, L., Ferreira, R., 2018. Multi-hazard analysis on the territory of the Coimbra municipality (western-central Portugal). The omnipresence of climate and the anthropic importance. Geo-Eco-Trop 41.

Curt, C., 2021. Multirisk: what trends in recent works? – a bibliometric analysis. Sci. Total Environ. 763, 142951 https://doi.org/10.1016/j.scitotenv.2020.142951.

Cutter, S.L., Boruff, B.J., Shirley, W.L., 2003. Social vulnerability to environmental hazards. Soc. Sci. Q. 84, 242–261.

Dąbrowska, J., Menéndez Orellana, A.E., Kilian, W., Moryl, A., Cielecka, N., Michałowska, K., Policht-Latawiec, A., Michalski, A., Bednarek, A., Włóka, A., 2023. Between flood and drought: how cities are facing water surplus and scarcity. J. Environ. Manag. 345, 118557 https://doi.org/10.1016/j.jenvman.2023.118557.

Dale, V.H., Joyce, L.A., McNulty, S., Neilson, R.P., Ayres, M.P., Flannigan, M.D., Hanson, P.J., Irland, L.C., Lugo, A.E., Peterson, C.J., Simberloff, D., Swanson, F.J., Stocks, B.J., Wotton, B.M., 2001. Climate Change and Forest Disturbances: climate change can affect forests by altering the frequency, intensity, duration, and timing of fire, drought, introduced species, insect and pathogen outbreaks, hurricanes, windstorms, ice storms, or landslides. Bioscience 51, 723–734. https://doi.org/10.1641/0006-3568(2001)051[0723:CCAFD]2.0.CO;2.

D'Amato Avanzi, G., Galanti, Y., Giannecchini, R., 2013. Fragility of Territory and Infrastructures Resulting from Rainstorms in Northern Tuscany (Italy). https://doi.org/10.1007/978-3-642-31319-6_33.

Dawson, R.J., Dickson, M.E., Nicholls, R.J., Hall, J.W., Walkden, M.J.A., Stansby, P.K., Mokrech, M., Richards, J., Zhou, J., Milligan, J., Jordan, A., Pearson, S., Rees, J., Bates, P.D., Koukoulas, S., Watkinson, A.R., 2009. Integrated analysis of risks of coastal flooding and cliff erosion under scenarios of long term change. Clim. Change 95, 249–288. https://doi.org/10.1007/s10584-008-9532-8.

Demir, V., Kisi, O., 2016. Flood hazard mapping by using geographic information system and hydraulic model: mert river, Samsun, Turkey. Advances in Meteorology 2016 1–9. https://doi.org/10.1155/2016/4891015.

Dessai, S., 2003. Heat stress and mortality in Lisbon Part II. An assessment of the potential impacts of climate change. Int. J. Biometeorol. 48, 37–44. https://doi.org/10.1007/s00484-003-0180-4.

Dottori, F., Alfieri, L., Bianchi, A., Skoien, J., Salamon, P., 2021. River Flood Hazard Maps for Europe and the Mediterranean Basin Region, Joint Research Centre (JRC), European Commission. https://doi.org/10.2905/1D128B6C-A4EE-4858-9E34-6210707F3C81PID. http://data.europa.eu/89h/1d128b6c-a4ee-4858-9e34-6210707f3c81.

Elia, L., Castellaro, S., Dahal, A., Lombardo, L., 2023. Assessing multi-hazard susceptibility to cryospheric hazards: lesson learnt from an Alaskan example. Sci. Total Environ. 898, 165289 https://doi.org/10.1016/j.scitotenv.2023.165289.

Espinosa, L.A., Portela, M.M., 2022. Grid-point rainfall trends, teleconnection patterns, and regionalised droughts in Portugal (1919–2019). Water (Basel) 14. https://doi.org/10.3390/w14121863.

Espinosa, L.A., Portela, M.M., Matos, J.P., Gharbia, S., 2022. Climate change trends in a European coastal metropolitan area: rainfall, temperature, and extreme events (1864–2021). Atmosphere 13. https://doi.org/10.3390/atmos13121995.

European Commission, Joint Research Centre (JRC), 2021. GDO Standardized Precipitation Index GPCC, 3-month Accumulation Period (SPI-3) [WWW Document], European Commission, Joint Research Centre (JRC) PID, version 1.2.0. http://data.europa.eu/89h/dca55d34-9151-419d-9366-5d64c28a4e07.

Eurosion, 2004. Available online at: [WWW Document]. URL www.eurosion.org (accessed 10.February.2023).

Faik, A., Sesli, F., 2010. Mapping and monitoring temporal changes for coastline and coastal area by using aerial data images and digital photogrammetry: a case study from Samsun,. Int. J. Phys. Sci. 5, 1567–1575.

Fang, J., Lincke, D., Brown, S., Nicholls, R.J., Wolff, C., Merkens, J.-L., Hinkel, J., Vafeidis, A.T., Shi, P., Liu, M., 2020. Coastal flood risks in China through the 21st century – an application of DIVA. Sci. Total Environ. 704, 135311 https://doi.org/10.1016/j.scitotenv.2019.135311.

Forzieri, G., Cescatti, A., e Silva, F.B., Feyen, L., 2017. Increasing risk over time of weather-related hazards to the European population: a data-driven prognostic study. Lancet Planet. Health 1, e200–e208. https://doi.org/10.1016/S2542-5196(17)30082-7.

Frazier, T.G., Thompson, C.M., Dezzani, R.J., Butsick, D., 2013. Spatial and temporal quantification of resilience at the community scale. Appl. Geogr. 42, 95–107. https://doi.org/10.1016/j.apgeog.2013.05.004.

Gallina, V., Torresan, S., Critto, A., Sperotto, A., Glade, T., Marcomini, A., 2016. A review of multi-risk methodologies for natural hazards: consequences and challenges for a

climate change impact assessment. J. Environ. Manag. 168, 123–132. https://doi.org/10.1016/j.jenvman.2015.11.011.
Gallina, V., Torresan, S., Zabeo, A., Critto, A., Glade, T., Marcomini, A., 2020. A multi-risk methodology for the assessment of climate change impacts in coastal zones. Sustainability 12. https://doi.org/10.3390/su12093697.
García, I., Negro, V., López, J.S., Esteban, M.D., Campo, J.M. del, 2020. Coastal morphological response to the effects of protection structures against erosion. J. Coast Res. 95 (1), 220–224. https://doi.org/10.2112/SI95-043.
García-Herrera, R., Garrido-Perez, J., Barriopedro, D., Ordonez, C., Vicente-Serrano, S., Nieto, R., Gimeno, L., Sorí, R., Yiou, P., 2019. The European 2016/17 Drought.
Garner, G.G., Hermans, T., Kopp, R.E., Slangen, A.B.A., Edwards, T.L., Levermann, A., Nowikci, S., Palmer, M.D., Smith, C., Fox-Kemper, B., Hewitt, H.T., Xiao, C., Aðalgeirsdóttir, G., Drijfhout, S.S., Edwards, T.L., Golledge, N.R., Hemer, M., Krinner, G., Mix, A., Notz, D., Nurhati, I.S., Ruiz, L., Sallée, J.-B., Yu, Y., Hua, L., Palmer, T., Pearson, B., 2021. IPCC AR6 Sea-Level rise projections [WWW Document]. URL. https://podaac.jpl.nasa.gov/announcements/2021-08-09-Sea-level-projections-from-the-IPCC-6th-Assessment-Report, 7.27.23.
Genovese, E.C.L., DeRoo, A., Barredo, J., Niemeyer, S., San-Miguel-Ayanz, J., Hiederer, R., Camia, A., 2005. Towards an European integrated map of risk from weather driven events: a contribution to the evaluation of territorial cohesion in Europe. https://publications.jrc.ec.europa.eu/repository/handle/JRC31950.
Ghorai, D., Sen, H.S., 2015. Role of climate change in increasing occurrences oceanic hazards as a potential threat to coastal ecology. Nat. Hazards 75, 1223–1245. https://doi.org/10.1007/s11069-014-1368-0.
Gill, J.C., Malamud, B.D., 2014. Reviewing and visualizing the interactions of natural hazards. Rev. Geophys. 52, 680–722. https://doi.org/10.1002/2013RG000445.
Godwyn-Paulson, P., Jonathan, M.P., Rodríguez-Espinosa, P.F., Abdul Rahaman, S., Roy, P.D., Muthusankar, G., Lakshumanan, C., 2022. Multi-hazard risk assessment of coastal municipalities of Oaxaca, Southwestern Mexico: an index based remote sensing and geospatial technique. Int. J. Disaster Risk Reduc. 77, 103041 https://doi.org/10.1016/j.ijdrr.2022.103041.
Gornitz, V., 1991. Global coastal hazards from future sea level rise. Palaeogeogr. Palaeoclimatol. Palaeoecol. 89, 379–398. https://doi.org/10.1016/0031-0182(91)90173-O.
Günther, A., Van Den Eeckhaut, M., Malet, J.-P., Reichenbach, P., Hervás, J., 2014. Climate-physiographically differentiated Pan-European landslide susceptibility assessment using spatial multi-criteria evaluation and transnational landslide information. Geomorphology 224, 69–85. https://doi.org/10.1016/j.geomorph.2014.07.011.
Gupta, A.K., Negi, M., Nandy, S., Kumar, M., Singh, V., Valente, D., Petrosillo, I., Pandey, R., 2020. Mapping socio-environmental vulnerability to climate change in different altitude zones in the Indian Himalayas. Ecol. Indicat. 109, 105787 https://doi.org/10.1016/j.ecolind.2019.105787.
Hersbach, H., Bell, B., Berrisford, P., Hirahara, S., Horányi, A., Muñoz-Sabater, J., Nicolas, J., Peubey, C., Radu, R., Schepers, D., Simmons, A., Soci, C., Abdalla, S., Abellan, X., Balsamo, G., Bechtold, P., Biavati, G., Bidlot, J., Bonavita, M., De Chiara, G., Dahlgren, P., Dee, D., Diamantakis, M., Dragani, R., Flemming, J., Forbes, R., Fuentes, M., Geer, A., Haimberger, L., Healy, S., Hogan, R.J., Hólm, E., Janisková, M., Keeley, S., Laloyaux, P., Lopez, P., Lupu, C., Radnoti, G., de Rosnay, P., Rozum, I., Vamborg, F., Villaume, S., Thépaut, J.-N., 2020. The ERA5 global reanalysis. Q. J. R. Meteorol. Soc. 146, 1999–2049. https://doi.org/10.1002/qj.3803.
Hong, J.-W., Hong, J., 2016. Changes in the seoul metropolitan area urban heat environment with residential redevelopment. J. Appl. Meteorol. Climatol. 55, 1091–1106. https://doi.org/10.1175/JAMC-D-15-0321.1.
Hooyberghs, H., Berckmans, J., Lefebre, F., De Ridder, K., 2019. Heat waves and cold spells in Europe derived from climate projections. Copernicus Climate Change Service (C3S) Climate Data Store (CDS). https://doi.org/10.24381/cds.9e7ca677 [WWW Document].
Hosseinzadehtalaei, P., Tabari, H., Willems, P., 2020. Climate change impact on short-duration extreme precipitation and intensity–duration–frequency curves over Europe. J. Hydrol. (Amst.) 590, 125249. https://doi.org/10.1016/j.jhydrol.2020.125249.
Howard, T., Palmer, M.D., Bricheno, L.M., 2019. Contributions to 21st century projections of extreme sea-level change around the UK. Environ Res Commun 1, 095002. https://doi.org/10.1088/2515-7620/ab42d7.
Intergovernmental Panel on Climate Change (IPCC), 2023. Ocean, cryosphere and Sea Level change. In: Climate Change 2021 – the Physical Science Basis: Working Group I Contribution to the Sixth Assessment Report of the Intergovernmental Panel on Climate Change. Cambridge University Press, Cambridge, pp. 1211–1362. https://doi.org/10.1017/9781009157896.011.
IPCC, 2021. Climate Change 2021: the Physical Science Basis. Contribution of Working Group I to the Sixth Assessment Report of the Intergovernmental Panel on Climate Change. Cambridge University Press, Cambridge, United Kingdom and New York, NY, USA (in press).
Irene, P., Paolo, V., Donatella, V., Alberto, M.J., Mauro, F., Giovanni, Z., 2010. Mapping the environmental risk of a tourist harbor in order to foster environmental security: objective vs. subjective assessments. Mar. Pollut. Bull. 60, 1051–1058. https://doi.org/10.1016/j.marpolbul.2010.01.021.
Ishida, K., Kavvas, M.L., Chen, Z.Q.R., Dib, A., Diaz, A.J., Anderson, M.L., Trinh, T., 2018. Physically based maximum precipitation estimation under future climate change conditions. Hydrol. Process. 32, 3188–3201. https://doi.org/10.1002/hyp.13253.
J Bergillos, R., Rodriguez-Delgado, C., Iglesias, G., 2019. Coastal flooding on gravel-dominated beaches under global warming. Global J. Environ. Sci. 1 https://doi.org/10.33552/GJES.2019.01.000513.
Kappes, M.S., Keiler, M., von Elverfeldt, K., Glade, T., 2012. Challenges of analyzing multi-hazard risk: a review. Nat. Hazards 64, 1925–1958. https://doi.org/10.1007/s11069-012-0294-2.
Keighley, T., Longden, T., Mathew, S., Trück, S., 2018. Quantifying catastrophic and climate impacted hazards based on local expert opinions. J. Environ. Manag. 205, 262–273. https://doi.org/10.1016/j.jenvman.2017.08.035.
Khojasteh, D., Chen, S., Felder, S., Glamore, W., Hashemi, M.R., Iglesias, G., 2022. Sea level rise changes estuarine tidal stream energy. Energy 239, 122428. https://doi.org/10.1016/j.energy.2021.122428.
Klein, R.J.T., Nicholls, R.J., 1999. Assessment of coastal vulnerability to climate change. Ambio 28, 182–187.
Knutson, T.R., McBride, J.L., Chan, J., Emanuel, K., Holland, G., Landsea, C., Held, I., Kossin, J.P., Srivastava, A.K., Sugi, M., 2010. Tropical cyclones and climate change. Nat. Geosci. 3, 157–163. https://doi.org/10.1038/ngeo779.
Kopp, R., Garner, G., Hermans, T., Jha, S., Kumar, P., Slangen, A., Turilli, M., Edwards, T., Gregory, J., Koubbe, G., Levermann, A., Merzky, A., Nowicki, S., Palmer, M., Smith, C., 2023. The Framework for Assessing Changes To Sea-level (FACTS) v1.0-rc: A platform for characterizing parametric and structural uncertainty in future global, relative, and extreme sea-level change. https://doi.org/10.5194/egusphere-2023-14.
Kovats, S., Valentini, R., Bouwer, L., Georgopoulou, E., Jacob, D., Martin, E., Rounsevell, M., Soussana, J.-F., 2014. Europe, 1267–1326. https://doi.org/10.1017/CBO9781107415386.003.
Kulp, S.A., Strauss, B.H., 2019. New elevation data triple estimates of global vulnerability to sea-level rise and coastal flooding. Nat. Commun. 10, 4844. https://doi.org/10.1038/s41467-019-12808-z.
Laino, E., Iglesias, G., 2023a. Extreme climate change hazards and impacts on European coastal cities: a review. Renew. Sustain. Energy Rev. 184, 113587 https://doi.org/10.1016/j.rser.2023.113587.
Laino, E., Iglesias, G., 2023b. Scientometric review of climate-change extreme impacts on coastal cities. Ocean Coast Manag. 242, 106709 https://doi.org/10.1016/j.ocecoaman.2023.106709.
Laino, E., Iglesias, G., 2023c. High-level characterisation and mapping of key climate-change hazards in European coastal cities. Nat. Hazards. https://doi.org/10.1007/s11069-023-06349-4.
Lang, A., Mikolajewicz, U., 2020. Rising extreme sea levels in the German Bight under enhanced CO2 levels: a regionalized large ensemble approach for the North Sea. Clim. Dynam. 55, 1829–1842. https://doi.org/10.1007/s00382-020-05357-5.
Laurien, F., Martin, J.G.C., Mehryar, S., 2022. Climate and disaster resilience measurement: persistent gaps in multiple hazards, methods, and practicability. Clim Risk Manag 37, 100443. https://doi.org/10.1016/j.crm.2022.100443.
Lavalle, C., Barredo, J., Roo, A., Feyen, L., Niemeyer, S., Camia, A., Hiederer, R., Barbosa, P., 2006. Pan European assessment of weather driven natural risks. In: Conference Proceedings: the EU Regional Policy Online Magazine. European Commission, DG Regio; 2006, pp. 1–12. JRC35044.
Lavaysse, C., Cammalleri, C., Dosio, A., van der Schrier, G., Toreti, A., Vogt, J., 2018. Towards a monitoring system of temperature extremes in Europe. Nat. Hazards Earth Syst. Sci. 18, 91–104. https://doi.org/10.5194/nhess-18-91-2018.
Le Gal, M., Fernández Montblanc, T., Montes Pérez, J., Duo, E., Souto Ceccon, P.E., Cabrita, P., Ciavola, P., 2022. ECFAS Pan-EU Flood Catalogue, D5.4 – Pan-EU flood maps catalogue - ECFAS project (GA 101004211). https://www.ecfas.eu/. https://doi.org/10.5281/zenodo.7488978.
Le Gal, M., Fernández-Montblanc, T., Duo, E., Montes Perez, J., Cabrita, P., Souto Ceccon, P., Gastal, V., Ciavola, P., Armaroli, C., 2023. A new European coastal flood database for low–medium intensity events. Nat. Hazards Earth Syst. Sci. 23, 3585–3602. https://doi.org/10.5194/nhess-23-3585-2023.
Lenôtre, N., Thierry, P., Batkowski, D., Vermeersch, F., 2004. EUROSION Project the Coastal Erosion Layer WP 2.6 BRGM/PC-52864-FR, p. 45, 8 fig., 3 app.
Lima, C.O., Bonetti, J., 2020. Bibliometric analysis of the scientific production on coastal communities' social vulnerability to climate change and to the impact of extreme events. Nat. Hazards 102, 1589–1610. https://doi.org/10.1007/s11069-020-03974-1.
Lin-Ye, J., García-León, M., Gràcia, V., Ortego, M.I., Lionello, P., Conte, D., Pérez-Gómez, B., Sánchez-Arcilla, A., 2020. Modeling of future extreme storm surges at the NW mediterranean coast (Spain). Water (Basel). https://doi.org/10.3390/w12020472.
Lionello, P., Barriopedro, D., Ferrarin, C., Nicholls, R., Orlic, M., Raicich, F., Reale, M., Umgiesser, G., Vousdoukas, M., Zanchettin, D., 2021. Extreme floods of Venice: characteristics, dynamics, past and future evolution (review article). Nat. Hazards Earth Syst. Sci. 21, 2705–2731. https://doi.org/10.5194/nhess-21-2705-2021.
Liu, X., Guo, P., Tan, Q., Xin, J., Li, Y., Tang, Y., 2019. Drought risk evaluation model with interval number ranking and its application. Sci. Total Environ. 685, 1042–1057. https://doi.org/10.1016/j.scitotenv.2019.06.260.
Lung, T., Lavalle, C., Hiederer, R., Dosio, A., Bouwer, L.M., 2013. A multi-hazard regional level impact assessment for Europe combining indicators of climatic and non-climatic change. Global Environ. Change 23, 522–536. https://doi.org/10.1016/j.gloenvcha.2012.11.009.
Luque, P., Gómez-Pujol, L., Marcos, M., Orfila, A., 2021. Coastal flooding in the balearic islands during the twenty-first century caused by Sea-Level rise and extreme events. Front. Mar. Sci. 8, 1052. https://doi.org/10.3389/fmars.2021.676452.
MacManus, K., Balk, D., Engin, H., McGranahan, G., Inman, R., 2021. Estimating population and urban areas at risk of coastal hazards, 1990–2015: how data choices matter. Earth Syst. Sci. Data 13, 5747–5801. https://doi.org/10.5194/essd-13-5747-2021.

Malakar, K., Mishra, T., Hari, V., Karmakar, S., 2021. Risk mapping of Indian coastal districts using IPCC-AR5 framework and multi-attribute decision-making approach. J. Environ. Manag. 294, 112948 https://doi.org/10.1016/j.jenvman.2021.112948.
Marosz, K., 2007. Studies on historical floods in Gdańsk (a methodological background). Geogr. Pol. 80, 111–116.
Martínez-Ibarra, E., 2015. Climate, water and tourism: causes and effects of droughts associated with urban development and tourism in Benidorm (Spain). Int. J. Biometeorol. 59, 487–501. https://doi.org/10.1007/s00484-014-0851-3.
McKee, T., Doesken, N., Kleist, J., 1993. The relationship of drought frequency and duration to time scales. In: Paper Presented at 8th Conference on Applied Climatology, vol. 17. Am. Meteorol. Soc., Anaheim, Calif.
Mclaughlin, S., Cooper, A., 2010. A Multi-scale coastal vulnerability index: a tool for coastal managers? Environ. Hazards 9, 233–248. https://doi.org/10.3763/ehaz.2010.0052.
Mercogliano, P., Rianna, G., Reder, A., Raffa, M., Mancini, M., Stojiljkovic, M., de Valk, C., van der Schrier, G., 2021. Extreme precipitation risk indicators for Europe and European cities from 1950 to 2019. Copernicus Climate Change Service (C3S) Climate Data Store (CDS). https://doi.org/10.24381/cds.3a9c4f89 [WWW Document].
Mitsopoulos, I., Chrysafi, I., Bountis, D., Mallinis, G., 2019. Assessment of factors driving high fire severity potential and classification in a Mediterranean pine ecosystem. J. Environ. Manag. 235, 266–275. https://doi.org/10.1016/j.jenvman.2019.01.056.
Mitsopoulos, I., Mallinis, G., 2017. A data-driven approach to assess large fire size generation in Greece. Nat. Hazards 88, 1591–1607. https://doi.org/10.1007/s11069-017-2934-z.
Murray, A.T., Carvalho, L., Church, R.L., Jones, C., Roberts, D., Xu, J., Zigner, K., Nash, D., 2021. Coastal vulnerability under extreme weather. Appl Spat Anal Policy 14, 497–523. https://doi.org/10.1007/s12061-020-09357-0.
Nardi, L., Rinaldi, M., 2015. Spatio-temporal patterns of channel changes in response to a major flood event: the case of the Magra River (central-northern Italy). Earth Surf. Process. Landforms 40, 326–339. https://doi.org/10.1002/esp.3636.
Neumann, B., Vafeidis, A.T., Zimmermann, J., Nicholls, R.J., 2015. Future coastal population growth and exposure to sea-level rise and coastal flooding–a global assessment. PLoS One 10, e0118571. https://doi.org/10.1371/journal.pone.0118571.
Nicholls, R., Klein, R., Tol, R., 2006. Managing Coastal Vulnerability and Climate Change: a National to Global Perspective.
Oppenheimer, M., Glavovic, B.C., Hinkel, J., van de Wal, R., Magnan, A.K., Abd-Elgawad, A., Cai, R., Cifuentes-Jara, M., DeConto, R.M., Ghosh, T., Hay, J., Isla, F., Marzeion, B., Meyssignac, B., Sebesvari, Z., 2019. Sea level rise and implications for low-lying islands, coasts and communities. In: Pörtner, H.-O., Roberts, D.C., Masson-Delmotte, V., Zhai, P., Tignor, M., Poloczanska, E., Mintenbeck, K., Alegría, A., Nicolai, M., Okem, A., Petzold, J., Rama, B.N.M., Weyer, N.M. (Eds.), IPCC Special Report on the Ocean and Cryosphere in a Changing Climate..
Ouyang, Z., Zheng, H., Xiao, Yi, Polasky, S., Liu, J., Xu, W., Wang, Q., Zhang, L., Xiao, Yang, Rao, E., Jiang, L., Lu, F., Wang, X., Yang, G., Gong, S., Wu, B., Zeng, Y., Yang, W., Daily, G.C., 2016. Improvements in ecosystem services from investments in natural capital. Science (1979) 352, 1455–1459. https://doi.org/10.1126/science.aaf2295.
Papathoma-Köhle, M., Promper, C., Glade, T., 2016. A common methodology for risk assessment and mapping of climate change related Hazards-Implications for climate change adaptation policies. Climate 4. https://doi.org/10.3390/cli4010008.
Paprotny, D., Terefenko, P., 2017. New estimates of potential impacts of sea level rise and coastal floods in Poland. Nat. Hazards 85, 1249–1277. https://doi.org/10.1007/s11069-016-2619-z.
Paranunzio, R., Anton, I., Adirosi, E., Ahmed, T., Baldini, L., Brandini, C., Giannetti, F., Meulenberg, C., Ortolani, A., Pilla, F., Iglesias, G., Gharbia, S., 2024. A new approach towards a user-driven coastal climate Service to enhance climate resilience in European cities. Sustainability 16. https://doi.org/10.3390/su16010335.
Paranunzio, R., Dwyer, E., Fitton, J.M., Alexander, P.J., O'Dwyer, B., 2021. Assessing current and future heat risk in Dublin city, Ireland. Urban Clim. 40, 100983 https://doi.org/10.1016/j.uclim.2021.100983.
Paranunzio, R., Guerrini, M., Dwyer, E., Alexander, P.J., O'Dwyer, B., 2022. Assessing coastal flood risk in a changing climate for Dublin, Ireland. J. Mar. Sci. Eng. 10 https://doi.org/10.3390/jmse10111715.
Paranunzio, R., Laio, F., Nigrelli, G., Chiarle, M., 2015. A method to reveal climatic variables triggering slope failures at high elevation. Nat. Hazards 76, 1039–1061. https://doi.org/10.1007/s11069-014-1532-6.
Petrosillo, I., Zurlini, G., Grato, E., Zaccarelli, N., 2006. Indicating fragility of socio-ecological tourism-based systems. Ecol. Indicat. 6, 104–113. https://doi.org/10.1016/j.ecolind.2005.08.008.
Pourghasemi, H.R., Gayen, A., Panahi, M., Rezaie, F., Blaschke, T., 2019. Multi-hazard probability assessment and mapping in Iran. Sci. Total Environ. 692, 556–571. https://doi.org/10.1016/j.scitotenv.2019.07.203.
Pryor, S.C., Barthelmie, R.J., Clausen, N.E., Drews, M., MacKellar, N., Kjellström, E., 2012. Analyses of possible changes in intense and extreme wind speeds over northern Europe under climate change scenarios. Clim. Dynam. 38, 189–208. https://doi.org/10.1007/s00382-010-0955-3.
Ranasinghe, R., Ruane, A.C., Vautard, R., Arnell, N., Coppola, E., Cruz, F.A., Dessai, S., Islam, A.S., Rahimi, M., Ruiz Carrascal, D., Sillmann, J., Sylla, M.B., Tebaldi, C., Wang, W., Zaaboul, R., 2021. Climate change information for regional impact and for risk assessment. In: Masson-Delmotte, V., Zhai, P., Pirani, A., Connors, S.L., Péan, C., Berger, S., Caud, N., Chen, Y., Goldfarb, L., Gomis, M.I., Huang, M., Leitzell, K., Lonnoy, E., Matthews, J.B.R., Maycock, T.K., Waterfield, T., Yelekçi, O., Yu, R., Zho, B. (Eds.), Climate Change 2021: the Physical Science Basis. Contribution of Working Group I to the Sixth Assessment Report of the Intergovernmental Panel on Climate Change. Cambridge University Press.
Rivas, V., Remondo, J., Bonachea, J., Sánchez-Espeso, J., 2020. Rainfall and weather conditions inducing intense landslide activity in northern Spain (Deba, Guipúzcoa). null 1–21. https://doi.org/10.1080/02723646.2020.1866790.
Rodriguez, D., Young, H., 2006. An Easy to Compute Index for Identifying Built Environments that Support Walking.
Rodriguez-Delgado, C., Bergillos, R.J., Iglesias, G., 2020. Coastal infrastructure operativity against flooding – a methodology. Sci. Total Environ. 719, 137452 https://doi.org/10.1016/j.scitotenv.2020.137452.
Rosendahl Appelquist, L., Balstrøm, T., 2015. Application of a new methodology for coastal multi-hazard-assessment & management on the state of Karnataka, India. J. Environ. Manag. 152, 1–10. https://doi.org/10.1016/j.jenvman.2014.12.017.
Rusk, J., Maharjan, A., Tiwari, P., Chen, T.-H.K., Shneiderman, S., Turin, M., Seto, K.C., 2022. Multi-hazard susceptibility and exposure assessment of the hindu kush himalaya. Sci. Total Environ. 804, 150039 https://doi.org/10.1016/j.scitotenv.2021.150039.
Sacchi, A., 2012. Meteorological analysis of floods between northern tuscany and eastern liguria from 2009 to 2011. Atti della Societa Toscana di Scienze Naturali 117–119, 75–88.
Sahoo, B., Bhaskaran, P.K., 2018. Multi-hazard risk assessment of coastal vulnerability from tropical cyclones – a GIS based approach for the Odisha coast. J. Environ. Manag. 206, 1166–1178. https://doi.org/10.1016/j.jenvman.2017.10.075.
Salvia, M., Reckien, D., Pietrapertosa, F., Eckersley, P., Spyridaki, N.-A., Krook-Riekkola, A., Olazabal, M., De Gregorio Hurtado, S., Simoes, S.G., Geneletti, D., Viguié, V., Fokaides, P.A., Ioannou, B.I., Flamos, A., Csete, M.S., Buzasi, A., Orru, H., de Boer, C., Foley, A., Rižnar, K., Matosović, M., Balzan, M.V., Smigaj, M., Baštáková, V., Streberova, E., Šel, N.B., Coste, L., Tardieu, L., Altenburg, C., Lorencová, E.K., Orru, K., Wejs, A., Feliu, E., Church, J.M., Grafakos, S., Vasilie, S., Paspaldzhiev, I., Heidrich, O., 2021. Will climate mitigation ambitions lead to carbon neutrality? An analysis of the local-level plans of 327 cities in the EU. Renew. Sustain. Energy Rev. 135, 110253 https://doi.org/10.1016/j.rser.2020.110253.
Sánchez-Almodóvar, E., Olcina-Cantos, J., Martí-Talavera, J., Prieto-Cerdán, A., Padilla-Blanco, A., 2023. Floods and adaptation to climate change in tourist areas: management experiences on the coast of the province of alicante (Spain). Water (Basel) 15. https://doi.org/10.3390/w15040807.
Santos, J.F., Pulido-Calvo, I., Portela, M.M., 2010. Spatial and temporal variability of droughts in Portugal. Water Resour. Res. 46 https://doi.org/10.1029/2009WR008071.
Sardella, A., Palazzi, E., Hardenberg, J., Grande, C., De Nuntiis, P., Sabbioni, C., Bonazza, A., 2020. Risk mapping for the sustainable protection of cultural heritage in extreme changing environments. Atmosphere 11, 700. https://doi.org/10.3390/atmos11070700.
Serafim, M.B., Siegle, E., Corsi, A.C., Bonetti, J., 2019. Coastal vulnerability to wave impacts using a multi-criteria index: santa Catarina (Brazil). J. Environ. Manag. 230, 21–32. https://doi.org/10.1016/j.jenvman.2018.09.052.
Skougaard Kaspersen, P., Høegh Ravn, N., Arnbjerg-Nielsen, K., Madsen, H., Drews, M., 2017. Comparison of the impacts of urban development and climate change on exposing European cities to pluvial flooding. Hydrol. Earth Syst. Sci. 21, 4131–4147. https://doi.org/10.5194/hess-21-4131-2017.
Tansel, B., 1995. Natural and manmade disasters: accepting and managing risks. Saf. Sci. 20, 91–99. https://doi.org/10.1016/0925-7535(94)00070-J.
Thakur, D.A., Mohanty, M.P., 2023. A synergistic approach towards understanding flood risks over coastal multi-hazard environments: appraisal of bivariate flood risk mapping through flood hazard, and socio-economic-cum-physical vulnerability dimensions. Sci. Total Environ. 901, 166423 https://doi.org/10.1016/j.scitotenv.2023.166423.
Tiwari, A., Rodrigues, L.C., Lucy, F.E., Gharbia, S., 2022. Building climate resilience in coastal city living Labs using ecosystem-based adaptation: a systematic review. Sustainability 14. https://doi.org/10.3390/su141710863.
Toledo, I., Pagán, J.I., López, I., Aragonés, L., 2022. Causes of the different behaviour against erosion: study case of the Benidorm Beaches (1956–2021). Mar. Georesour. Geotechnol. 1–14. https://doi.org/10.1080/1064119X.2022.2084003.
Trinh, T., Ishida, K., Kavvas, M.L., Ercan, A., Carr, K., 2017. Assessment of 21st century drought conditions at Shasta Dam based on dynamically projected water supply conditions by a regional climate model coupled with a physically-based hydrology model. Sci. Total Environ. 586, 197–205. https://doi.org/10.1016/j.scitotenv.2017.01.202.
Tu, T., Carr, K.J., Ercan, A., Trinh, T., Kavvas, M.L., Nosacka, J., 2017. Assessment of the effects of multiple extreme floods on flow and transport processes under competing flood protection and environmental management strategies. Sci. Total Environ. 607–608, 613–622. https://doi.org/10.1016/j.scitotenv.2017.06.271.
Ülke Keskin, A., Demir, V., Beden, N., 2018. Analysis of annual, seasonal and monthly trends of climatic data: a case study of Samsun. Nat. Sci. 13, 51–70.
Vicente-Serrano, S.M., Quiring, S.M., Peña-Gallardo, M., Yuan, S., Domínguez-Castro, F., 2020. A review of environmental droughts: increased risk under global warming? Earth Sci. Rev. 201, 102953 https://doi.org/10.1016/j.earscirev.2019.102953.
VijayaVenkataRaman, S., Iniyan, S., Goic, R., 2012. A review of climate change, mitigation and adaptation. Renew. Sustain. Energy Rev. 16, 878–897. https://doi.org/10.1016/j.rser.2011.09.009.
Vousdoukas, M.I., Mentaschi, L., Voukouvalas, E., Verlaan, M., Feyen, L., 2017. Extreme sea levels on the rise along Europe's coasts. Earth's Future 5, 304–323. https://doi.org/10.1002/2016EF000505.
Wang, J., He, Z., Weng, W., 2020. A review of the research into the relations between hazards in multi-hazard risk analysis. Nat. Hazards 104, 2003–2026. https://doi.org/10.1007/s11069-020-04259-3.

Wilde, M., Günther, A., Reichenbach, P., Malet, J.-P., Hervás, J., 2018. Pan-European landslide susceptibility mapping: ELSUS Version 2. J. Maps 14, 97–104. https://doi.org/10.1080/17445647.2018.1432511.

Wiśniewski, B., Wolski, T., Musielak, S., 2011. A long-term trend and temporal fluctuations of the sea level at the Polish Baltic coast. Oceanological and Hydrobiological Studies - OCEANOL HYDROBIOL STUD 40, 96–107. https://doi.org/10.2478/s13545-011-0020-9.

WMO, 2012. Standardized Precipitation Index User Guide.

Wong, P.P., Losada, I.J., Gattuso, J.-P., Hinkel, J., Khattabi, A., McInnes, K.L., Saito, Y., Sallenger, A., 2014. Coastal systems and low-lying areas. In: Field, C.B., Barros, V.R., Dokken, D.J., Mach, K.J., Mastrandrea, M.D., Bilir, T.E., Chatterjee, M., Ebi, K.L., Estrada, Y.O., Genova, R.C., Girma, B., Kissel, E.S., Levy, A.N., MacCracken, S., Mastrandrea, P.R., White, L.L. (Eds.), Climate Change 2014: Impacts, Adaptation, and Vulnerability. Part A: Global and Sectoral Aspects. Contribution of Working Group II to the Fifth Assessment Report of the Intergovernmental Panel on Climate Change. Cambridge University Press, Cambridge, United Kingdom and New York, NY, USA, pp. 361–409.

Yamazaki, D., Ikeshima, D., Tawatari, R., Yamaguchi, T., O'Loughlin, F., Neal, J.C., Sampson, C.C., Kanae, S., Bates, P.D., 2017. A high-accuracy map of global terrain elevations. Geophys. Res. Lett. 44, 5844–5853. https://doi.org/10.1002/2017GL072874.

Yan, K., Muis, S., Irazoqui, M., Verlaan, M., 2020. Water level change indicators for the European coast from 1977 to 2100 derived from climate projections. Copernicus Climate Change Service (C3S) Climate Data Store (CDS). https://doi.org/10.24381/cds.b6473cc1 [WWW Document].

Zhang, S., Zhang, J., Li, X., Du, X., Zhao, T., Hou, Q., Jin, X., 2023. Quantitative risk assessment of typhoon storm surge for multi-risk sources. J. Environ. Manag. 327, 116860 https://doi.org/10.1016/j.jenvman.2022.116860.